SEMMELWEIS EGYETEM

DOKTORI ISKOLA

Ph.D. értekezések

3529.

SZŐCS EMŐKE

Embriológia, őssejt és fejlődésbiológia
című program

Programvezető: Dr. Nagy Nándor, egyetemi tanár
Témavezető: Dr. Nagy Nándor, egyetemi tanár

Characterization of cellular and extracellular regulators of lymphoid organogenesis in the developing bursa of Fabricius

PhD thesis

Emőke Szőcs

Semmelweis University Doctoral School

Molecular Medicine Division

Supervisor: Nándor Nagy, D.Sc

Official reviewers: Péter Balogh, D.Sc

Zoltán Péter Jakus, Ph.D, Habil.

Head of the Complex Examination Committee:

Attila Mócsai, D.Sc

Members of the Complex Examination Committee:

Elen Gócza, D.Sc

Zoltán Péter Jakus, Ph.D, Habil.

Budapest

2026

TABLE OF CONTENTS

LIST OF ABBREVIATIONS 3
1. INTRODUCTION 4
1.1. The bursa of Fabricius, a model to study B cell development - past and present ... 5
1.2. Structure of the bursa of Fabricius 6
1.3. Morphogenesis of bursal lymphoid follicles 8
1.3.1. First stage: Development of the bursal rudiment and initiation of follicle bud formation 8
1.3.2. Second stage: cortex formation and B cell emigration to the periphery 12
1.4. The role of lymphoid tissue inducer cells in secondary lymphoid organogenesis 14
2. OBJECTIVES 17
3. METHODS 18
3.1. Animals 18
3.2. Immunohistochemistry 18
3.3. Immunofluorescence 19
3.4. Electron microscopy 22
3.5. RNAscope *in situ* hybridization 23
3.6. Chemical bursectomy with testosterone-propionate treatment 23
3.7. Chorioallantoic membrane transplantation 24
3.8. Epithelial-mesenchymal tissue recombination experiments 24
3.9. *Shh*-RCAS retrovirus-mediated perturbation 25
3.10. *In vitro* B cell migration assay 25
3.11. B cell adhesion assay 26
3.12. Statistical analysis 26
4. RESULTS 27
4.1. Developmental mechanism of lymphoid follicle formation and characterization of bursal lymphoid follicle inducer cells 27
4.1.1. Hematopoietic colonization of the bursa of Fabricius 27
4.1.2. CD45+/EIV-E12+ cells colonize the bursal epithelium 29

4.1.3. Follicle bud formation coincides with the colonization of EIV-E12+/*CSF1R*-eGFP- cells to the epithelium 31
4.1.4. EIV-E12+ cells do not give rise to dendritic cells or B cells 33
4.1.5. Follicle bud induction occurs independently of dendritic cell and B cell precursors 36
4.1.6. EIV-E12+ cells induce follicle bud formation 39
4.2. Development of the lymphoid follicular cortex and mechanisms of cortical B cell emigration 41
4.2.1. Characterization of lymphoid follicles in the chicken bursa of Fabricius 41
4.2.2. The cortex is rich in extracellular matrix proteins 43
4.2.3. Complementary expression of tenascin-C and CXCR4 in the follicular cortex 45
4.2.4. Expression of tenascin-C in the embryonic bursa of Fabricius 46
4.2.5. Shh-induced overexpression of tenascin-C disrupts lymphoid follicle formation 48
4.2.6. *In vitro* B cell migration is inhibited by tenascin-C 50
4.2.7. CXCL12-Tenascin-C interactions influence B cell morphology 52
5. DISCUSSION 53
6. CONCLUSION 62
7. SUMMARY 63
8. REFERENCES 64
9. BIBLIOGRAPHY OF THE CANDIDATE'S PUBLICATIONS 75
9.1. List of publications related to the thesis 75
9.2. List of own publications not related to the thesis 76
10. ACKNOWLEDGMENTS 79

LIST OF ABBREVIATIONS

BF	bursa of Fabricius
BSDC	bursal secretory dendritic cell
CAM	chorioallantoic membrane
CSF1R	Colony Stimulating Factor 1 Receptor
CXCL12	C-X-C motif chemokine Ligand type 12
CXCL13	C-X-C motif chemokine Ligand type 13
CXCR4	C-X-C motif chemokine Receptor type 4
CXCR5	C-X-C motif chemokine Receptor type 5
DAPI	4,6 diamidino-2-phenylindole
E	embryonic day
ECM	extracellular matrix
EdU	5-ethynyl-2'-deoxyuridine
FAE	follicle-associated epithelium
GFP	green fluorescent protein
ILC	innate lymphoid cell
LTi	lymphoid tissue inducer
LTo	lymphoid tissue organizer
MALT	mucosa-associated lymphoid tissue
RCAS	replication-competent avian retrovirus
Shh	Sonic hedgehog
SLO	secondary lymphoid organ
TIM4	T-cell immunoglobulin and mucin domain-containing 4

1. INTRODUCTION

The vertebrate immune system is a highly interconnected network of lymphoid organs, immune cells, and molecular factors that are indispensable for the immune homeostasis of an individual. The complex response to pathogens is generated in specialized lymphoid organs, harbouring unique microenvironments, that eventually leads to the formation of immunological memory, making the vertebrate immune system very effective in tackling a wide range of pathogens and quickly adapting to modified environmental factors. Understanding these processes at the cellular and molecular level has been the focus of immunology and developmental biology research for decades, and immunological model organisms have had an indispensable role in uncovering these complex mechanisms.

Before the wide availability of transgenic technologies in rodents, fundamental discoveries were made using the avian model system, which shaped modern immunology. The discovery of graft-versus-host reaction and antibody-producing B cells in the bursa of Fabricius in the first half of the 19th century sparked a number of scientific questions and resulted in breakthrough discoveries. The search for mammalian, bursa-equivalent organs led to the delineation of the two branches of the adaptive immune system: T cell-dependent cellular immunity and B cell-dependent humoral immunity, one of the fundamental principles that shaped modern immunology. The unique features of the avian embryo made it an exceptional vertebrate model system to study early hematopoiesis, making it particularly useful in assessing inductive capacities of cell-cell interactions and understanding early lymphoid organ and B cell development, a process that occurs isolated from other lymphoid, myeloid, and erythroid lineages.

Despite having in-depth knowledge of B cell function and cellular interactions, microenvironmental factors that drive B cell development and differentiation require further investigation. Long-term maintenance of B cells *in vitro,* especially the capacity to support mature B cell proliferation, poses significant challenges. Current techniques for primary B cell culture limit clonal expansion of cells to a few weeks and do not support mature B cell proliferation. In addition, some B cell types are still hard to culture as they depend on several factors and cell-cell interactions for their survival and growth. Hybridization with immortal

myeloma cells or retroviral transduction of B cells aids long-term maintenance, but these techniques drastically alter B cell physiology, making them unfit for functional studies that could be easily translated into *in vivo* systems. Understanding B cell biology and the complex molecular interactions during embryogenesis that lead to the formation of functional cells will advance our understanding of the intricate workings of the immune system and eventually contribute to the development of more effective stem cell therapies for hematologic disorders.

1.1. The bursa of Fabricius, a model to study B cell development - past and present

Uncovering the mechanisms by which the adaptive immune system recognizes and efficiently eliminates the multitude of foreign molecules has long been the focus of immunology. The concept of recognizing pathogens by antibodies was first introduced by Paul Ehrlich at the beginning of the 19th century (Zipfel and Skerka, 2022), and their production was linked to plasma cells by Astrid Fagreaus in 1947, based on his immunization experiments in rabbits (Fagraeus, 1947). The identity of the antibody-producing cells and their origin, however, puzzled scientists for the following decades, and the discovery that shaped modern immunology came by chance and involved the peculiar cloaca-associated organ of birds, the bursa of Fabricius. The organ was first described by Hieronymus Fabricius of Aquapendente in 1621, who, based on its anatomical location, associated it with the storage of semen. Often referred to as the "cloacal thymus", it was later associated with having endocrine function, influencing sexual maturation of birds. The identification of bursal function came only after 350 years of its original discovery, when bursectomized chickens were used in a routine experiment to produce antibodies against *Salmonella typhimurium* O antigen, and the results showed a complete lack of antibodies in these birds (Glick et al., 1956). After several experiments, Glick et al. were the first to show that the bursa of Fabricius plays a crucial role in the immunocompetence of birds, via antibody production. With the discovery of the immunological role of the thymus through xenografting experiments in the following years (Miller, 1961), it became apparent that the immune system uses distinct lymphocyte populations to perform specialized roles in recognizing foreign antigens. The

delineation of thymus-derived, T cell-mediated immune responses and bursa-derived B cell-mediated humoral immunity eventually came through breakthrough experiments, performed in chickens to show that bursectomized animals fail to develop germinal centers, plasma cells, or antibodies but exhibit normal cellular immune functions and foreign skin graft rejection. Similarly, removing the thymus severely impacts cellular immunity but has only mild effects on antibody production (Cooper et al., 1965). These findings led to the delineation of cellular and humoral immunity, the two branches of the adaptive immune system, which have shaped modern immunology. After this initial discovery, several bursa-equivalent organs have been described in mammals, like the ileal Peyer's patches in ruminants, the appendix in rabbits, and the bone marrow in humans and rodents (Abdou and Abdou, 1972; Abdou and Richter, 1970; Pospisil and Mage, 2011; Reynaud et al., 1991; Yasuda et al., 2006). Characterizing the specialized microenvironment that drives proliferation, differentiation, and diversification of the antibody repertoire of B cells has been the focus of immunology ever since and using the bursa of Fabricius to complement mammalian studies has been crucial to understanding the complexity of the immune system.

1.2. Structure of the bursa of Fabricius

The bursa of Fabricius (BF) is a unique avian-specific primary lymphoid organ that is the central site of B cell development in birds. The organ has the size and shape of a chestnut and is connected to the proctodeal region of the cloaca by a bursal duct (Cooper et al., 1965; Glick et al., 1956; Nagy et al., 2022). Proliferation and differentiation of B cells occur in the bursal lymphoid follicles, which are considered the basic structural and functional units of the organ and are organized in 10-12 longitudinal folds. Each fold is covered by two types of surface epithelium: pseudostratified interfollicular epithelium (IFE) and follicle-associated epithelium (FAE) (Nagy et al., 2001; Olah and Glick, 1978). The FAE connects the bursal lumen with bursal lymphoid follicles and is the functional equivalent of mammalian M-cells, allowing antigens to pass from the external environment directly into the medulla of bursal follicles (Balic et al., 2019). Each follicle consists of a central medullary region, separated by a basement membrane from the cortex, which develops around hatch

and reaches its final maturity two weeks post-hatch. These structurally well-separated compartments each retain unique lymphoid, myeloid, and stromal cells that provide a specialized microenvironment to support different stages of B cell maturation.

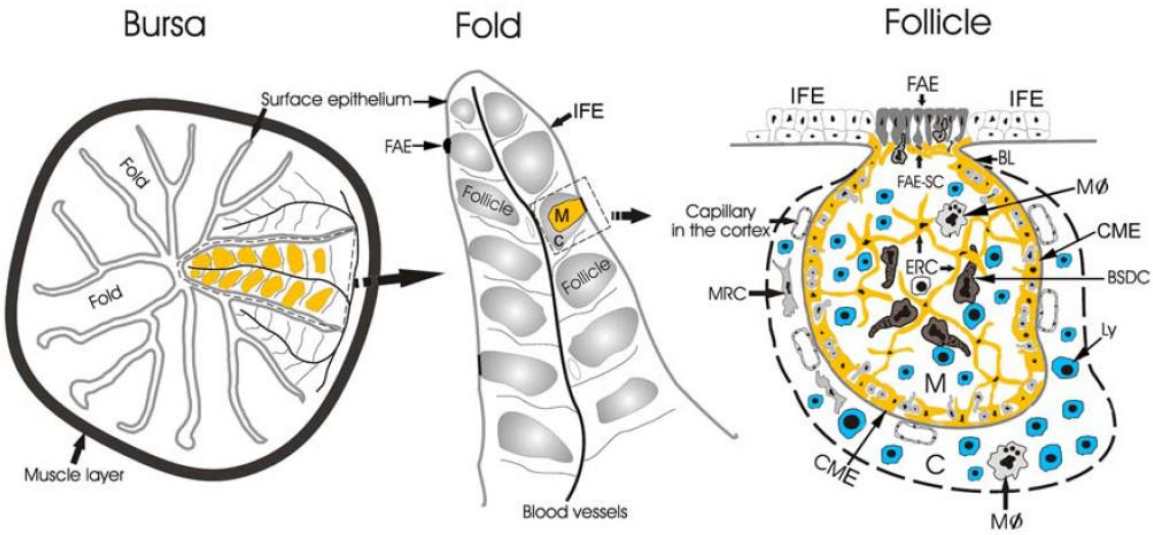


Figure 1. Schematic representation of bursal structure. Bursal lymphoid follicles (yellow) fill the axis of bursal folds. Individual follicles are divided into a medulla and a cortex, separated by a basement membrane. M: medulla, C: cortex, FAE: follicle-associated epithelium, IFE: interfollicular epithelium, FAE-SC: follicle-associated epithelium supporting cell, BL: basal lamina, ERC: epithelial reticular cell, MRC: mesenchymal reticular cell, CME: cortico-medullary epithelium, Ly: lymphocyte, BSDC: bursal secretory dendritic cell, MØ: macrophage (Nagy et al., 2022).

The BF reaches its maximum size 4-8 weeks after hatching, which coincides with intense lymphopoietic activity, followed by a gradual involution after sexual maturity. During involution, lympho-epithelial bursal follicles are gradually replaced by connective tissue (Ciriaco et al., 2003). As the bursa loses its characteristic tissue structure, adaptive immune functions in adult birds rely on long-lived bursa-derived B cells that migrate to extra-bursal sites and populate secondary lymphoid organs (Lassila, 1989; Paramithiotis and Ratcliffe, 1993; Ratcliffe, 2006; von La Roche et al., 2024). Generation of the antibody diversity in birds by gene conversion occurs exclusively in bursal lymphoid follicles (McCormack et al.,

1991; Thompson and Neiman, 1987), which makes the BF a valuable model to study the microenvironmental factors required for the ontogeny of B cells. While it is believed that the bone-marrow harbours a population of post-bursal stem cells as an alternative source of B cells after bursal involution, the bone-marrow microenvironment can only facilitate Ig gene rearrangement, without the capacity to induce gene conversion, a process indispensable for the generation of the antibody diversity in birds (Benatar et al., 1991; Mansikka et al., 1990; Ratcliffe, 2006; Reynaud et al., 1987; Toivanen and Toivanen, 1973).

1.3. Morphogenesis of bursal lymphoid follicles

1.3.1. First stage: Development of the bursal rudiment and initiation of follicle bud formation

Chicken BF development can be characterized by two distinct morphogenetic events during embryogenesis, which result in the formation of lympho-epithelial follicle buds with the capacity to support B cell proliferation and maturation. First, the bursal rudiment appears by an epithelial-mesenchymal interaction, a process which begins at embryonic day (E)4.5-5 at the endodermal-ectodermal border of the cloacal plate. The epithelial anlage of the BF is of ectodermal origin and arises as a diverticulum of the cloacal epithelium, that starts growing into the tail bud mesenchyme (Nagy and Oláh, 2010). By E8, a well-defined bursal lumen forms, lined by the surface epithelium, which is surrounded by a loose network of undifferentiated tail bud mesenchyme. Further specification of the epithelio-mesenchymal rudiment into bursal lymphoid follicles relies on immigrating blood-borne cells, a process which occurs between E8-E15 in a sequential manner (Houssaint, 1987; Le Douarin et al., 1975; Masteller et al., 1995; Nagy et al., 2004b; Oláh et al., 1986).

Pre-bursal stem cells colonizing the BF rudiment arise from the definitive wave of hematopoiesis, associated with the ventral wall of the dorsal aorta (Dieterlen Lievre, 1975; Jaffredo et al., 2000). RUNX1+/c-kit+ clusters of cells emerge from the hemogenic endothelium by a process called endothelial to hematopoietic transition (EHT). These cells form intra-aortic hematopoietic clusters (IAHCs) that are a common feature of definitive hematopoiesis in almost all vertebrate embryos (Yvernogeau and Robin, 2017). In mice and

humans, 500-700 definitive HSCs migrate to the fetal liver, where they undergo limited expansion but acquire functional maturity and robust bone marrow engraftment ability (Christensen et al., 2004; Ganuza et al., 2017). In contrast, IAHC cells in avian embryos are transiently found in the loose mesenchyme ventral to the aorta between E6-E9, where they form the para-aortic foci as a final expansion site before colonizing the definitive hematopoietic organs (Fig.2) (Dóra et al., 2017; Dunon et al., 1998).

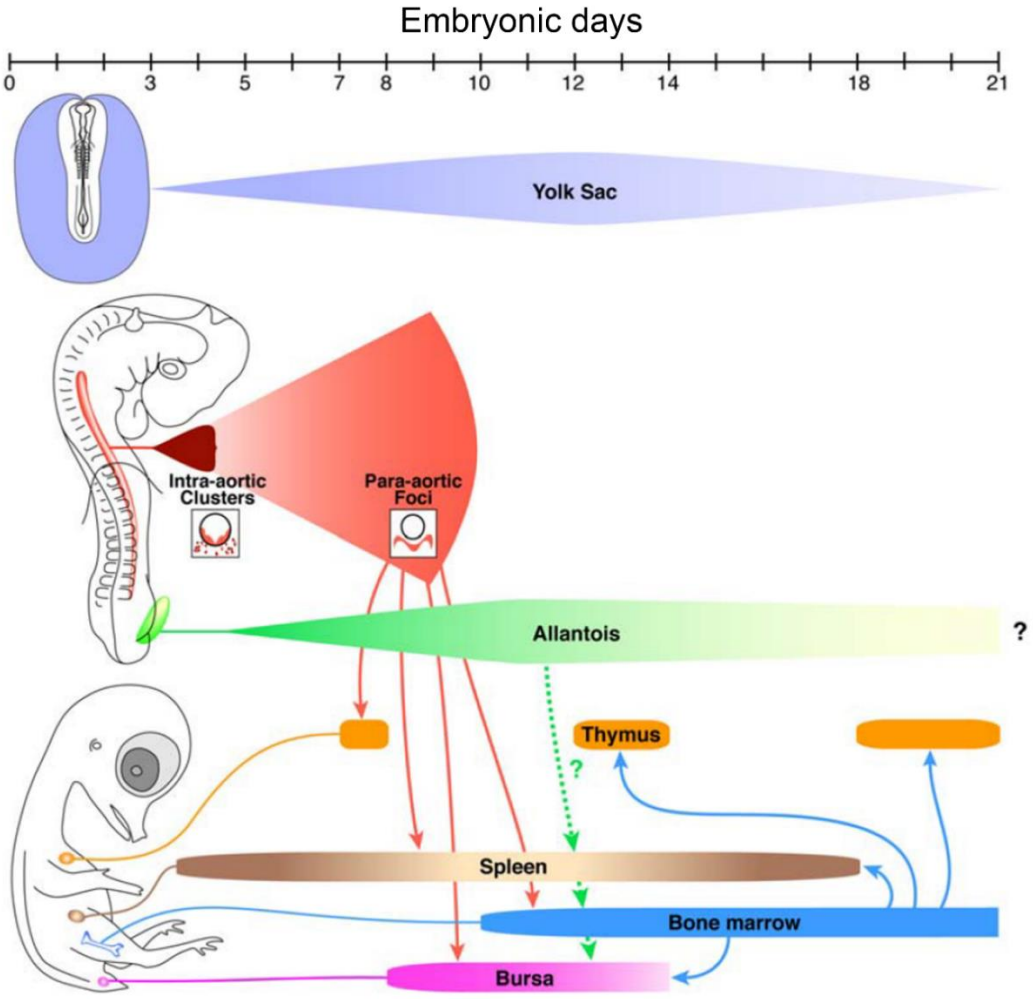


Figure 2. Schematic representation of embryonic hematopoiesis and lymphoid organ colonization in birds. The primary sites of embryonic hematopoiesis include the yolk sac, intra-aortic hematopoietic clusters, para-aortic foci and allantois. Among lymphoid organs, colonization of the spleen is initiated first, followed by the thymus, the bursa of Fabricius, and subsequently the bone marrow (Yvernogeau et al., 2022).

First incoming cells that colonize the bursal anlage are indifferent for the morphogenesis of lymphoid follicles and are a population of CD45+/Grl1+/Grl2+ granulocytes that support the granulopoietic activity of the organ until hatch (Nagy et al., 2020; Quesada and Agulleiro, 1984). Granulocytes are never found within lymphoid follicles, and bursal granulopoiesis ceases before hatching.

The next population of CD45+ cells colonizes the bursa mesenchyme at E9, shows a highly ramified morphology, and reaches the surface epithelium by E10-11 (Dóra et al., 2017; Nagy et al., 2004a; Nagy et al., 2004b). They express the colony-stimulating factor-1 receptor (CSF1R) and the major histocompatibility complex II (MHCII) antigen and cross the basement membrane of the epithelium (Dóra et al., 2017). After initial clustering in the surface epithelium, they start expressing vimentin intermediate filaments, CD11c, and dendritic cell-specific 74.3 antigen (Houssaint, 1987; Nagy et al., 2004b; Oláh and Nagy, 2013; Oláh et al., 1986) and are considered the precursors of bursal secretory dendritic cells (BSDCs). Invasion of the CSF1R+/MHCII+/vimentin+/74.3+/CD11c+ BSDCs in the surface epithelium is considered the initiation step of follicle bud formation. While it is widely accepted that epithelial follicle bud formation relies on the invasion of BSDCs in the surface epithelium, the earliest studies characterizing bursal follicle formation first identified this population of cells solely based on their intense basophilic staining by toluidine blue (Oláh et al., 1986). Determining the origin and fate of these “dark cells” resulted in three contradictory hypotheses identifying this population as EIV-E12+ precursors of BSDCs, precursors of the follicle-associated epithelium, or myeloid cells of the macrophage lineage (Lupetti et al., 1990; Nagy et al., 2004b; Shiojiri and Takahashi, 1991).

Emergence of epithelial follicle buds is a continuous process between E11-E15 (Nagy et al., 2001). Pre-bursal stem cells committed to the B cell lineage first appear in the bursal mesenchyme starting from E10 and colonize the epithelial follicle buds by E13 (Nagy et al., 2004b; Nagy et al., 2020). These bursal B cell precursors originate from intra-embryonic hematopoietic sites and have undergone somatic gene rearrangement in extra-bursal sites, such as the bone marrow or the embryonic spleen, express surface IgM, chB6, and CXCR4 (Mansikka et al., 1990; McCormack et al., 1989; Nagy et al., 2020; Reynaud et al., 1994). Between E9-E10, the bursal mesenchyme is a major source of the CXCL12 chemokine,

which guides these chB6+/IgM+/CXCR4+ cells to the bursal rudiment. Upon emergence of the dendro-epithelial tissue, CXCL12 expression gradually shifts to the epithelial follicle buds, and the first B cells are detected within the follicles starting from E13 (Laparidou et al., 2020; Nagy et al., 2020). Each follicle bud is initially colonized by 3-4 B lymphocyte precursors, which begin a phase of rapid proliferation, that is the major driver of lymphoid follicle formation (Pink et al., 1985; Weill et al., 1986). The extensive proliferation and survival of B cells are likely driven by an evolutionarily conserved mechanism that involves CD40 and BAFF ligands. Bursal B cells express the CD40 and BAFF-receptors, and *in vitro* experiments reported increased proliferation and survival in ligand-stimulated B cell cultures (Kothlow et al., 2006; Kothlow et al., 2008; Schneider et al., 2004).

Diversification of the B cell antibody repertoire starts between E15-E17 within bursal follicles through repeated somatic gene conversion events, a process that occurs exclusively in bursal lymphoid follicles (Ratcliffe, 2006; Reynaud et al., 1987). While mammals generate their diverse antibody repertoire by somatic gene rearrangement and have several genes encoding the variable (V), joining (J) and diversity (D) regions for both Ig heavy (H) and light (L) chains, chickens have only one functional V_L and V_H segment, and gene rearrangement provides almost no diversity (Parvari et al., 1988; Reynaud, 1985). To compensate for having only one functional gene, chickens possess a large reservoir of pseudogenes located upstream of the functional V_H and V_L segments. During gene conversion, a process driven by the activation-induced cytidine deaminase (AID) enzyme, homologous sequences from upstream pseudogenes are recombined into the rearranged V segment, which results in the generation of an antibody repertoire similar to mammals (Arakawa and Buerstedde, 2004; Reynaud et al., 1989). While Ig gene rearrangement is a continuous process in mammalian species, birds generate the antibody repertoire by gene conversion during a short period in late-embryonic and early adult life, and this process occurs exclusively in bursal lymphoid follicles (McCormack et al., 1989; McCormack et al., 1991; Thompson and Neiman, 1987). Perturbations of the early stages of bursa development highlight its indispensable role in generating the antibody repertoire. Surgical or chemical bursectomy by testosterone propionate treatment results in the development of bursaless birds, which are severely immunocompromised (Nagy and Oláh, 2009; Oláh et al., 1986;

Wilson and Boyd, 1990). These animals show a significantly reduced number of B cells, produce only a restricted antibody repertoire, and are generally not able to initiate specific antibody responses by isotype switching to IgG or IgA (Kowalski et al., 1978; Masteller and Thompson, 1994). This confirms that while some B cells can reach the periphery without a bursa, the typical maturation and selection processes that allow a functional, diverse B cell population are essentially lost.

1.3.2. Second stage: cortex formation and B cell emigration to the periphery

At the time of hatching, epithelial follicles undergo a second morphogenetic event, leading to the compartmentalization of the follicles into medulla and cortex. This process is initiated by the migration of B cells from the epithelial follicle buds to the surrounding mesenchyme, where they establish a distinct population of B cells that proliferate between desmin+ mesenchymal cells surrounding the epithelial follicles (Sayegh et al., 2000). While the chB6 antigen is expressed uniformly by all bursal B cells, cortical and medullary populations show significant morphological and immunophenotypical differences. Cortical B cells are usually smaller, show higher levels of proliferation compared to the medulla, and are positive for the LT2, CD80, and CXCR4 antigens (Lee et al., 2011; Nagy et al., 2020; Paramithiotis and Ratcliffe, 1994). In contrast, surface IgM expression is observed only in medullary B cells (Olah et al., 1992). While the medulla shows the characteristic features of a classical lympho-epithelial tissue, the cortex has a connective tissue framework of mesenchymal origin. B cells and macrophages are organized around desmin+/vimentin+ mesenchymal reticular cells that produce a network of extracellular matrix (ECM) proteins rich in collagens, fibronectin, and laminin (Oláh and Nagy, 2013). Importantly, CSF1R+/74.3+/vimentin+ bursal secretory dendritic cells are not present in the cortex of lymphoid follicles (Balic et al., 2019; Nagy et al., 2016a) and the cortical myeloid cell population consists of TIM4+/LEP100+ macrophages.

Based on these significant structural differences, the cortex of adult lymphoid follicles is thought to have fundamentally different functional roles than the medulla. From hatching until involution, active migration of B cells can be observed between the medulla and the

cortex. It is believed that the bursa gives rise to two distinct populations of adult B cells that reach the periphery. About 90% of recent bursal emigrants originate from rapidly proliferating cells in the cortex that express the LT2 antigen (Paramithiotis and Ratcliffe, 1996). Bromodeoxyuridine (BrdU) pulse-chase experiments show that BrdU-labeled cells are detected in the peripheral blood before they appear in the follicular medulla, demonstrating that most bursal emigrants leave directly from the cortex (Paramithiotis and Michael, 1994). This population consists of naive, short-lived cells that have not been selected by environmental antigens and disappear within three days. In contrast, long-lived peripheral blood B cell populations do not express the LT2 antigen and represent a functionally distinct population that has undergone selection within the follicular medulla by antigens derived from the gut lumen (Ratcliffe, 2006). These antigen-selected B cells eventually migrate to the periphery along cortical capillaries (Madej et al., 2013; Paramithiotis and Michael, 1994; Paramithiotis and Ratcliffe, 1993).

Bursal B cell emigration is a complex, multi-step process that involves several migratory steps, from medulla to cortex and cortex to blood circulation, but the mechanisms that control these migration steps remain largely unknown. Previous studies examining bursal function primarily focused on the ontogeny and role of the follicular medulla in B cell development, leaving the bursal follicular cortex a neglected part. Recent studies highlighted the role of the CXCR4-CXCL12 signaling in guiding B cells from the medulla to the CXCL12-rich cortical microenvironment (Nagy et al., 2020). It is currently hypothesized that for these cortical B cells to enter the blood circulation, they must downregulate CXCR4 expression to escape chemokine-mediated retention (Nagy et al., 2020). However, the specific regulatory mechanisms within the cortex that orchestrate this final migratory step have yet to be fully elucidated.

1.4. The role of lymphoid tissue inducer cells in secondary lymphoid organogenesis

A key evolutionary innovation of the vertebrate immune system is the presence of adaptive immunity and the emergence of specialized anatomical regions where immune cell activation can occur with high efficiency (Boehm, 2025; Neely and Flajnik, 2016). Secondary lymphoid organs (SLOs) play a crucial role in appropriate immune function, and in mammals and humans, these include the spleen, peripheral and mesenteric lymph nodes, and the mucosa-associated lymphoid tissue (MALT). Although these SLOs exhibit numerous structural similarities, such as well-defined B and T cell compartments, their ontogeny relies on distinct cell-cell and molecular interactions. These processes are primarily orchestrated by specialized cells, first described by Mebius et al. (1997) as cell lineage marker negative CD45+/CD3-/CD4+/LTβ+ cells. Upon transplantation, these cells significantly increased the number of Peyer's patches and have been termed lymphoid tissue inducer (LTi) cells (Finke et al., 2002; Meier et al., 2007). Since their original discovery, several other lymphocyte populations having innate-like functions have been identified, and together these were termed innate lymphoid cells (ILCs) (Das et al., 2026; Eberl et al., 2015; Vivier et al., 2018). They represent an evolutionarily ancient population that has a primary role in providing rapid, tissue-specific immune responses, bridging innate and adaptive immune functions. ILCs are tissue-resident immune cells that lack diversified antigen-specific receptors, integrate environmental signals, and respond by heavy cytokine secretion, resembling T-helper (Th) functions (Gasteiger et al., 2015). Based on their signature transcription factor expression, ILCs were originally divided into three groups. ILC1s are defined by the expression of T-bet and have important functions in tackling tumors and intracellular pathogens. ILC2s are characterized by GATA3 expression and are primarily involved in immune responses against extracellular parasites, while ILC3s are defined by the expression of RORγt and constitute a heterogeneous population. They are important in maintaining gut homeostasis, having a critical role in preserving the epithelial barrier and containing commensal bacteria within the gastrointestinal tract. Based on the dependence of RORγt expression, LTi cells were also defined as ILC3 cells (Vivier et al., 2018).

ILC development progresses from common lymphoid progenitors (CLP) in the fetal liver and continues in the adult bone marrow, through intermediate populations characterized

by distinct transcription factor profiles, such as all-lymphoid progenitor (ALP), NFIL3+ lymphoid precursors (NLP), early-innate lymphoid progenitor (EILP), and innate lymphoid cell precursors (ILCP) (Cherrier et al., 2012; Das et al., 2026; Klose et al., 2014). Based on detailed transcriptomic analyses, NK-cells were later defined as a divergent member of the ILC1 family, dependent on the expression of the EOMES transcription factor. While all other ILC populations rely on the expression of PLZF and originate from ILCPs, LTis do not require the PLZF transcription factor for their development, and they diverge much earlier (Constantinides et al., 2014; Das et al., 2026). LTi cell commitment in the fetal liver is marked by the expression of *Rorc* in α-lymphoid progenitors (α-LP) and represents an abundant population during embryogenesis, but is rare in the adult bone marrow (Kasal and Bendelac, 2021). LTi cells have a half-life of 22-26 days, and as fetal hematopoiesis transitions to bone marrow-derived adult hematopoiesis, fetal LTi cells are gradually replaced by bone marrow-derived counterparts (Sawa et al., 2010).

Further maturation occurs as LTi progenitors migrate to peripheral sites, where retinoic acid induces the expression of RORγt, and immature LTi cells transition to a committed state marked by the expression of CD4, IL-7Rα, CCR6, and CXCR5 receptors (Simic et al., 2020; van de Pavert et al., 2014). At the onset of secondary lymphoid organ development, mature LTi cells utilize lymphotoxin ligands to interact with mesenchymal lymphoid tissue organizer cells (LTo) expressing the lymphotoxin-β receptor (LTβR) (Fütterer et al., 1998; Rennert et al., 1998). Lymphotoxin signaling induces the secretion of CXCL13 ligands in LTo cells, resulting in the recruitment of LTi cells, via the CXCR5-CXCL13 axis (Mebius, 2003; Van De Pavert et al., 2009). While both lymph node and Peyer's patch organogenesis are primarily driven by LTi-LTo cell interactions via lymphotoxin and CXCR5-CXCL13 chemokine signaling, mechanisms of LTi cell recruitment differ. The initial steps of Peyer's patch organogenesis rely on the activation of VCAM+ mesenchymal cells expressing RET ligands such as Artemin and Neurturin, which recruit CD45+/CD11c+/c-kit+/RET+ lymphoid tissue initiator cells (LTin) (Patel et al., 2012; Veiga-Fernandes et al., 2007). This initial interaction drives the differentiation of VCAM+ mesenchymal cells into CXCL13-expressing LTo cells, which in turn recruit CXCR5+/LTα1β2+ LTi cells to the Peyer's patch anlagen. In case of lymph node

development, the initial recruitment of LTi cells relies heavily on CCL21 expression by lymphatic endothelial cells, which, upon interaction, activate the non-canonical NF-κB signaling and are the major source of recruitment signals. Once LTi cell numbers reach a threshold, they induce the maturation of perivascular fibroblasts, leading to the upregulation of adhesion molecules and chemokines such as CXCL13, making them the LTo cells for lymph node development (Onder et al., 2017). While lymphotoxin signaling is crucial for the development of lymph nodes, different receptor-ligand interactions were identified to drive lymph node development in distinct anatomical regions: LTα3 is the major driver of mesenteric, cervical, and sacral lymph nodes, whereas the LTα1β2 ligand complex is specifically required for peripheral lymph node development (Koni et al., 1997; Ruddle, 2025).

While birds lack well-defined lymph nodes, they possess an extensive gut-associated lymphoid tissue network, with the bursa of Fabricius as a major site of early B cell development. Studies investigating the development of primary and secondary lymphoid organs in avian species do not mention populations analogous to lymphoid tissue inducer and organizer cells described in mammals, but recent data from B cell-deficient chicken model systems generated by CRISPR/Cas9-mediated RAG1 knockout (Lee et al., 2022) or the *in vivo* blockade of CXCR4 signaling (Nagy et al., 2020) show that follicle bud formation persists in the absence of B cells. The fact that follicle buds develop normally in these immunodeficient chickens implies the existence of a distinct inducer cell population that initiates lymphoid follicle formation before B cell colonization.

2. OBJECTIVES

The bursa of Fabricius serves as the primary lymphoid organ for avian B cell development, characterized by a complex stromal and cellular microenvironment and unique morphogenetic events during early embryogenesis. Despite having in-depth knowledge of B cell function and cellular interactions, microenvironmental factors that drive B cell development and differentiation require further investigation. Understanding the complex molecular interactions during embryogenesis that lead to the formation of B cell-specific competent niches is essential for understanding how functional immune cells reach maturity.

The primary objectives of this thesis are to:

1. Identify the lympho-myeloid stem cells driving the ontogenesis of lymphoid follicles in the bursa of Fabricius
2. Characterize the development, structure, and extracellular microenvironment in the cortex of adult lymphoid follicles

Our specific aims are to:

- Identify the lympho-myeloid and stromal cells that precede B cell precursors in early bursal colonization
- Map the fate of EIV-E12+ cells in lymphoid follicles using embryo manipulation techniques
- Characterize the lymphoid, myeloid, and stromal cells in the cortex of adult lymphoid follicles
- Characterize the expression of tenascin-C in the cortex of lymphoid follicles
- Elucidate the regulatory function of tenascin-C in B cell migration using embryo manipulation techniques and *in vitro* assays

3. METHODS

3.1. Animals

Fertilized White Leghorn chicken (*Gallus gallus domesticus*) eggs were obtained from commercial breeders (Prophyl-BIOVO Ltd., Hungary). Transgenic *CSF1R*-eGFP-expressing chicken eggs were obtained from the National Avian Research Facility at The Roslin Institute, University of Edinburgh. Production of the *CSF1R*-eGFP reporter transgenic line has been previously described (Balic et al., 2014). For epithelial-mesenchymal recombination experiments, quail (*Coturnix japonica domestica*) eggs were purchased from commercial breeders. For chorioallantoic membrane transplantation fertilized duck eggs (*Anas platyrhynchos domesticus*) were obtained from the National Center for Biodiversity and Gene Conservation, Institute for Farm Animal Gene Conservation, Gödöllő, Hungary. Eggs were maintained at 37.5°C in a humidified incubator, and embryos were staged according to the number of embryonic (E) days. Hatched animals were housed in the aviary of the Department of Anatomy, Histology and Embryology, Semmelweis University. All animal work was conducted according to relevant national and international guidelines and approved by the Animal Care and Use Committee at Semmelweis University, Budapest, Hungary.

3.2. Immunohistochemistry

After developmental staging, the bursa of Fabricius (BF) from E9-E13 chicken embryos and 2-8 weeks post-hatch chicken were fixed in 4% paraformaldehyde (PFA) for 1 hour at room temperature. Tissue samples were incubated in 15% sucrose overnight at 4°C, then infiltrated with phosphate-buffered saline (PBS) containing 7.5% gelatine and 15% sucrose for 2 hours at 37°C. Impregnated tissue samples were subsequently embedded in the same 7.5% gelatine medium and snap-frozen at -50°C in 2-methylbutane (Sigma, 78-78-4). Frozen gelatine blocks were sectioned by a Shandon cryotome, and 12 μm cryosections were mounted on poly-L-lysine (Sigma, P8920) coated slides. To visualize the expression of specific antigens, sections were incubated with primary antibodies (Table 1) for 1 hour at room temperature, followed by biotinylated secondary antibodies for 45 minutes (Table 2)

and avidin-biotinylated peroxidase complex for 30 minutes (ABC; Vectastain Elite ABC kit, Vector Laboratories, PK-6100). Endogenous peroxidase activity was quenched by 3% hydrogen-peroxide (Sigma, H1009) in PBS for 10 minutes. The binding sites of the primary antibodies were visualized by 4-chloro-1-naphthol (Sigma, C8890). Sections were covered by aqueous Poly/Mount (Polyscience Inc. Warrington, PA, 18606).

3.3. Immunofluorescence

For double immunofluorescence, gelatine-embedded 12 µm cryosections were rehydrated in warm PBS for 10 minutes. Sections were incubated with primary antibodies (Table 1) diluted in PBS, containing 1% bovine serum albumin (BSA) for 1 hour at room temperature, followed by incubation with Alexa-conjugated fluorescent secondary antibodies (Table 2) for 45 minutes at room temperature. Cell nuclei were counterstained with 4,6-diamidino-2-phenylindole (DAPI; Vector Labs, Burlingame, California) and sections were covered by aqueous Poly/Mount (Polyscience Inc., Warrington, PA, 18606). To assess cell proliferation, tissue samples were kept in Dulbeccos's Modified Eagles Medium (DMEM, Sigma, D6429) containing 10 µM 5-ethynyl-20-deoxyuridine (EdU) for three hours prior to fixation with 4% paraformaldehyde (PFA). EdU incorporation was subsequently detected using the Click-iT EdU Imaging Kit (Thermo Fisher, C10337). Sections were analyzed using epifluorescence (Nikon Eclipse E800), confocal laser scanning (Zeiss LSM 780) and stimulated emission depletion (STED; Abberior Expert Line- Nikon Ti2) microscopy. Images were acquired using CellSens and ZEISS ZEN software. Post-processing was performed using ImageJ and Adobe Photoshop CC 2020.

Table 1. List of primary antibodies

Antigen	Clone	Structure/cell identified	Dilution	Source of antibody	Isotype
CD45	HISC7	hematopoietic cells	1:200	Prionics Co.	mouse IgG_{2A}
CD4	CT-4	T cells	1:200	Southern Biotech	mouse IgG_1
CD3	CT-3	T cells	1:200	BioRad	mouse IgG_1

200 kDa glycoprotein	EIV-E12	lymphoid follicle inducer cells	supernatant	Dr. Todd Pharr (USA) (Pharr et al., 1995a)	mouse IgG_1
chB6 (Bu-1a/b)	BoA1	B cells	supernatant	BioRad (Igyártó et al., 2008)	mouse IgG_1
IgM	M2	B cells	1:200	Dr. Sonja Härtle, München University (Erhard et al., 1992)	mouse IgG_1
CXCR4	9D9	B cells, granulocytes	supernatant	Dr. Sonja Härtle, München University	mouse IgG_{2A}
BAFF-R	2C4	B cells	1:200	Dr. Sonja Härtle, München University	mouse IgG_1
CSF1R	ROS-AV-170	dendritic cells, macrophages	1:100	Dr. Zhiguang Wu, Roslin Institute (Garcia-Morales et al., 2014)	mouse IgG_1
TIM4	JH9	macrophage subsets	1:1000	Dr. Zhiguang Wu, Roslin Institute (Garcia-Morales et al., 2014)	mouse IgG_1
74.3	CVI-ChNL-74.3	chicken dendritic cells	1:50	Prionics	mouse IgG_1
MHCII	21-1A6	chicken major histocompatibility complex class II expressing antigen presenting cells	1:100	Thermo Fisher	mouse IgG_1
duck CD8	CD8-1	duck leukocytes	1:200	Dr. Sonja Härtle, München University (Kothlow et al., 2005)	mouse IgG_1
E-cadherin	36	epithelial cells	1:200	BD Biosciences	mouse IgG_{2A}
cytokeratin	Lu-5	epithelial cells	1:200	Millipore (MAB3406)	mouse IgG_1
Neuropilin-1	TB2	endothelial cells	supernatant	Developmental Studies Hybridoma Bank (DSHB)	mouse IgG_1
motor neuronal marker (SC-1)	BEN	bursa epithelium and neurons	supernatant	DSHB	mouse IgG_1

quail cell nuclear antigen	QCPN	all quail cells	supernatant	DSHB	mouse IgG_1
chicken cell cytoplasmic antigen	8F3-s	all chicken cells	supernatant	DSHB	mouse IgG_1
collagen I	SPID8	ECM	supernatant	DSHB	mouse IgG_1
collagen III	3B2	ECM	supernatant	DSHB	mouse IgG_1
collagen IV	IIB12	ECM	supernatant	DSHB	mouse IgG_1
collagen VI	5C6	ECM	supernatant	DSHB	mouse IgG_1
collagen XVIII	6C4	ECM	supernatant	DSHB	mouse IgG_1
laminin	3H11	ECM	supernatant	DSHB	mouse IgG_1
agrin	6D2	ECM	supernatant	DSHB	mouse IgG_1
fibronectin	B3/D6	ECM	supernatant	DSHB	mouse IgG_1
fibrillin	JC3	ECM	supernatant	DSHB	mouse IgG_1
perlecan	5C9	ECM	supernatant	DSHB	mouse IgG_1
versican	12C5-s	ECM	supernatant	DSHB	mouse IgG_1
podocalyxin	MEP21	chicken endothelial cells	1:200	Dr. Kelly McNagny, Canada (McNagny et al., 1997)	mouse IgG_1
vimentin	3B4	Intermediate filaments	1:50	Sigma	mouse IgG_{2A}
desmin	DE-R-11	Intermediate filaments	1:100	Santa Cruz Biotechnology	mouse IgG_1
tenascin-C	M1-B4	ECM	supernatant	DSHB	mouse IgG_1
Shh	5E1	extracellular Sonic hedgehog protein	1:100	DSHB	mouse IgG_1

avian myeloblastosis virus, p19^(gag)	3C2	p19^(gag) protein of the avian myeloblastosis virus	supernatant	DSHB	mouse IgG_1

Table 2. List of secondary antibodies

Secondary antibodies	Source	Catalog number
biotinylated anti-mouse IgG (H+L)	BioMarker Kft.	BA-9200
biotinylated anti-mouse IgM	BioMarker Kft.	BA-2020
biotinylated anti-rabbit IgG	BioMarker Kft.	BA-1000
Alexa Fluor 488 donkey anti-mouse IgG	Thermo Fisher Scientific	A-21202
Alexa Fluor 594 donkey anti-mouse IgG	Thermo Fisher Scientific	A-21203
Alexa Fluor 647 donkey anti-mouse IgG	Thermo Fisher Scientific	A-31571
Alexa Fluor 594 goat anti-mouse IgG_{2A}	Thermo Fisher Scientific	A-21135
Alexa Fluor 488 goat anti-mouse IgG2a	Thermo Fisher Scientific	A-21131
Alexa Fluor 488 goat anti-rabbit IgG	Thermo Fisher Scientific	A-32731

3.4. Electron microscopy

4-week-old chicken bursa of Fabricius were fixed in 4% buffered glutaraldehyde for 24 hours at 4°C, washed 3 times for 5 minutes in Milloning buffer (830ml 2.26% Na2HPO4 • 2H2O- Merck, 106462 and 170ml 2.52% NaOH - Merck, 1.06346.1000), then post-fixed with 1% osmium tetraoxide for 2 hours (Merck - B000970). For EIV-E12 immunoelectron-microscopy E10 bursa of Fabricius were fixed and embedded in 7.5% gelatine as described above. Gelatine cubes were postfixed in 4% paraformaldehyde for 48 hours at 4°C. 200 µm thick vibratome sections were collected and incubated overnight with EIV-E12 primary antibody using a free-floating technique. After extensive washing in PBS, sections were incubated with biotinylated goat anti-mouse IgG secondary antibody overnight at 4°C. The secondary antibody was followed by incubation with avidin-biotinylated peroxidase complex for 1 hour at room temperature (Vectastain Elite ABC kit, Vector Laboratories, PK-6100). Endogenous peroxidase activity was quenched with 3% hydrogen peroxide (Sigma, H1009).

EIV-E12 staining was visualized with 3,3-diaminobenzidine-NiSO4 (Sigma). Sections were postfixed in 4% glutaraldehyde for 24 hours at 4°C, followed by 1% osmium tetroxide (Polysciences Inc., Warrington, PA) for 2 hours at room temperature. Samples were dehydrated in graded ethanol and embedded in Polybed/Araldite 6500 (Polysciences Inc., Warrington, PA). After careful orientation tissue blocks were polymerized at 56 °C for 2 days. 1 µm semithin sections were collected on Epredia™ Superfrost Plus Adhesion Slides (Fisher Scientific, J1800AMNZ) and stained with toluidine blue. Ultrathin (60 nm) sections were contrasted with a mixture of uranyl acetate and lead citrate and imaged with a JEOL JEM-1200EX transmission electron microscope.

3.5. RNAscope *in situ* hybridization

Expression of the CXCL12 chemokine ligand was detected in isolated bursa of Fabricius from 4-week-old chicken. Dissected bursal folds were fixed in 4% PFA for 24 hours at 4°C, rinsed in PBS and dehydrated in graded series of 10%, 20% and 30% sucrose solutions overnight at 4°C. Tissues were then impregnated with 7.5% gelatine for two hours at 37.5°C, embedded in the same gelatine medium and snap-frozen at -50°C in 2-methylbutane. 12 µm thick cryosections were mounted on Epredia™ Superfrost Plus Adhesion Slides (Fisher Scientific, J1800AMNZ) and stored at -80°C until use. RNAscope was performed with the RNAscope Fluorescent Multiplex Detection Reagent Kit v2 (Bio-Techne, 323136) using a chicken-specific Gg-CXCL12-C2 probe (Bio-Techne, 458251) according to the manufacturer's protocol. To identify the source of the CXCL12 signal, RNAscope was followed by immunocytochemistry as described above.

3.6. Chemical bursectomy with testosterone-propionate treatment

Chemical bursectomy using testosterone-propionate treatment is a classical method in avian immunology used to suppress the earliest stages of BF development (Oláh et al., 1986). To assess the effects of chemical bursectomy on lymphoid follicle formation, fertilized White Leghorn chicken eggs were incubated for 24 hours at 37.5°C and dipped in 2,5% testosterone propionate (TP, Sigma, 57-85-2) dissolved in absolute ethanol (Molar Chemicals

Kft., 02910-101-340) for 5 seconds. Treated eggs were returned to the incubator, and embryos were allowed to develop *in ovo* for 14 days. BF from control and TP-treated embryos were isolated (n=8/group), fixed in 4% PFA, embedded in gelatine, and processed for immunohistochemistry.

3.7. Chorioallantoic membrane transplantation

To map the fate of EIV-E12+ cells within bursal lymphoid follicles, E9 chicken bursa of Fabricius were isolated in PBS containing 5% Penicillin/Streptomycin (Pen/Strep, Sigma, P0781) and transplanted onto the chorioallantoic membrane (CAM) of E11 duck embryos. To expose the richly vascularized CAM, the eggshell was carefully removed above the air cell and a drop of Pen/Strep-PBS was applied onto the inner shell membrane. By gently piercing the shell membrane, the sterile solution was allowed to penetrate between the CAM and the shell membrane, allowing the removal of the latter without damaging the underlying vasculature of the CAM. A small, Y-shaped vessel on the CAM was gently traumatized, and the BF primordia were placed directly onto it to promote engraftment. Eggs were sealed with adhesive tape and incubated at 37°C with 70% humidity for additional 7 and 11 days (n=8).

For CXCR4 signal blocking experiments 1 µl of 200 µM AMD3100 (Sigma, 239820) was injected into the mesenchymal wall of isolated E9 bursa primordia (Nagy et al., 2020). Grafts were transplanted onto the CAM of E9 chicken embryos and cultured for 9 days *in ovo* (n=9). Control grafts were prepared by injecting an equivalent volume of sterile Pen/Strep-PBS, used as solvent in the experimental samples (n=6). CAM grafts were excised, fixed in 4% PFA and embedded in gelatin for cryosectioning.

3.8. Epithelial-mesenchymal tissue recombination experiments

The follicle bud inducing capacity of EIV-E12+ cells was evaluated through a series of quail-chick epithelial-mesenchymal tissue recombination experiments. The BF epithelium of E8 quail embryos was recombined with mesenchyme of BF or hindgut origin isolated from E9 chicken embryos. Briefly, E8 quail BF primordium, E9 chicken BF primordium and E9 chicken hindgut were digested with 0.03% collagenase (Sigma, T1875) in Dulbeccos's Modified Eagles Medium (DMEM, Sigma, D6429) for 15 minutes at 37°C. Enzymatic

activity was blocked by three washing steps in fetal bovine serum (FBS, Sigma, F9665). The BF epithelium was isolated from the mesenchyme using fine forceps. In case of hindgut, the mesenchymal wall of the tissue was longitudinally opened, and the intestinal epithelium was removed with the help of a tungsten needle. To allow the tissues to adhere recombinants (Experiment 1: quail BF epithelium+chicken BF mesenchyme; Experiment 2: quail BF epithelium+chicken hindgut mesenchyme) were cultured on a layer of 3D-collagen gel matrix (Gibco, A10483). After overnight incubation, the recombinant chimeric tissues were removed from the collagen gel and transplanted onto the CAM of E9 chicken then cultured for 9 days. CAM grafts were excised, fixed in 4% PFA and embedded in gelatine for cryosectioning.

3.9. *Shh*-RCAS retrovirus-mediated perturbation

To induce ectopic expression of tenascin-C we used the replication-competent avian retrovirus (RCAS) expressing chick sonic-hedgehog (Shh) (Riddle et al., 1993). Shh misexpression in the developing chick bursa of Fabricius was performed by injecting 1 µl Shh-RCAS virus into the mesenchymal layer of the bursa of Fabricius of E9 chicken embryos. Shh-RCAS injected E9 bursa primordia were transplanted onto the chorioallantoic membrane of E9 chicken embryos and cultured *in ovo* for an additional 8 days (n=9). Control grafts were injected with equal amount of Pen/Strep-PBS (n=6). CAM grafts were excised and fixed in 4% PFA for 1 hour at room temperature, embedded in gelatine for cryosectioning. To assess the extent of the viral infection across the BF, the distribution of the viral vector was confirmed by 3C2 immunolabeling. Tissue sections were subsequently analyzed for Shh and tenascin-C expression.

3.10. *In vitro* B cell migration assay

To determine how different matrix molecules affect B cell migration, E13 bursal folds were dissected and explanted onto tissue culture dishes coated with 20 µg/ml fibronectin (Sigma, F1141) or 10 µg/ml tenascin-C (Sigma, CC115). ECM proteins were diluted in RPMI 1640 (Sigma, R8758), containing 5% Pen/Strep, and Petri dishes were incubated at 37 °C for 2 hours. To remove unbound proteins, culture dishes were washed twice with PBS. To

stimulate emigration of B cells, bursal folds were cultured in RPMI medium containing 5% Pen/Strep and 100 ng/ml CXCL12 (100 ng/ml; R&D Systems, 6448-SD-025) (n=6/experimental setup). Cultures were maintained at 37°C, under 5% CO_2 for 24 hours. Adherent cells were fixed in ice-cold 100% methanol for 20 minutes and immunolabeled to detect CXCR4+ bursal B cells.

3.11. B cell adhesion assay

Chicken bursal B cells were isolated from E18 embryos to evaluate tenascin-C-mediated adhesion. Briefly, E18 bursal folds were enzymatically digested with 0.03% collagenase IX (Sigma, C9722) and 2% dispase II (Stem Cell Technologies, 07913) diluted in RPMI 1640 medium (Sigma, R8758-500ML) for 30 minutes at 37°C with gentle agitation. The cell suspension was passed through a 40 µm cell strainer and washed twice in RPMI supplemented with 10% FBS (fetal bovine serum, Capricorn Scientific, FBS-12B) and 5% Pen/Strep. Cells were centrifuged at 1500 rpm for 8 minutes, resuspended in RPMI medium, and seeded at a density of 2×10^5 cells in tissue culture dishes coated with chicken tenascin-C (10 µg/ml) and CXCL12 (100 µg/ml; PeproTech, 250-20A). CXCR4 signaling was inhibited by treatment with the CXCR4 receptor antagonist AMD3100 (Sigma, 239820) at a concentration of 200 µM. Control cells were cultured in RPMI only. After 6 hours, non-adhesive cells were removed by gentle aspiration, and adherent cells were fixed in ice-cold 100% methanol for 20 minutes. All cell adhesion assays were repeated 3 times, and B cells were detected by anti-chB6 immunolabeling.

3.12. Statistical analysis

Statistical analysis was performed using the Mann–Whitney *U* test, Kruskal-Wallis test, or ANOVA with a post-hoc Dunn's test or Tukey test (R Core Team). P-values were adjusted with Holm correction. $P<0.05$ was considered significant, and the following significance levels were used: **p<0.01; ***p<0.001; ****p<0.0001. Violin plots presenting all data points and bar graphs were generated using the Graphpad Prism v9.4.1 proprietary software. Error bars represent the standard error of the mean or the median of all data points (further specified in the figure legends).

4. RESULTS

4.1. Developmental mechanism of lymphoid follicle formation and characterization of bursal lymphoid follicle inducer cells

4.1.1. Hematopoietic colonization of the bursa of Fabricius

To characterize the first incoming cells that colonize the bursa primordium and initiate bursal lymphoid organogenesis, we performed extensive immunostaining with a panel of lymphoid- and myeloid-specific markers and examined the blood-borne colonization of the bursa of Fabricius. The epithelial rudiment of the BF is first detectable at E7, as a cytokeratin+ sac-like outgrowth of the cloacal epithelium (Fig. 3A). The transition of the bursal epithelial-mesenchymal rudiment into a functional site for B cell differentiation depends on colonization by blood-borne cells, which occurs during a short developmental time window, between embryonic days (E)9 and 15. The CD45-specific antibody is a suitable tool for detecting all hematopoietic cells that express the common leukocyte antigen. While CD45 immunoreactive hematopoietic cells are uniformly scattered within the tail bud mesenchyme at E7 (Fig. 3B, C), they only begin to accumulate in the mesenchyme surrounding the bursal anlage by E8 (Fig. 3D-F). One day later, on E9, CD45+ cells show both ramified and round morphologies (Fig. 3H). Further phenotypic characterization with lymphoid- and myeloid-specific antibodies identified two distinct myeloid cell populations. Highly ramified cells that express the colony-stimulating factor-1 receptor (CSF1R) are the most abundant and are uniformly scattered throughout the mesenchyme (Fig. 3I). In contrast, the second population expresses the phosphatidylserine receptor TIM4, and cells are localized in the outer mesenchymal region of the bursa primordium (Fig. 3J).

At this developmental stage, cells committed to the lymphocyte lineage, characterized by the expression of lineage markers such as chB6 (Fig.3K), BAFF-R, CD4, or CD3, are not yet present (data not shown). While cells expressing B cell markers are absent, the EIV-E12 monoclonal antibody, which recognizes a 200 kDa membrane glycoprotein present on the surface of 90% of adult bursal cells, labels a unique population in the E9 BF mesenchyme. These EIV-E12 immunoreactive cells have a single, spike-like process and are frequently observed near the surface epithelium (Fig. 3L).

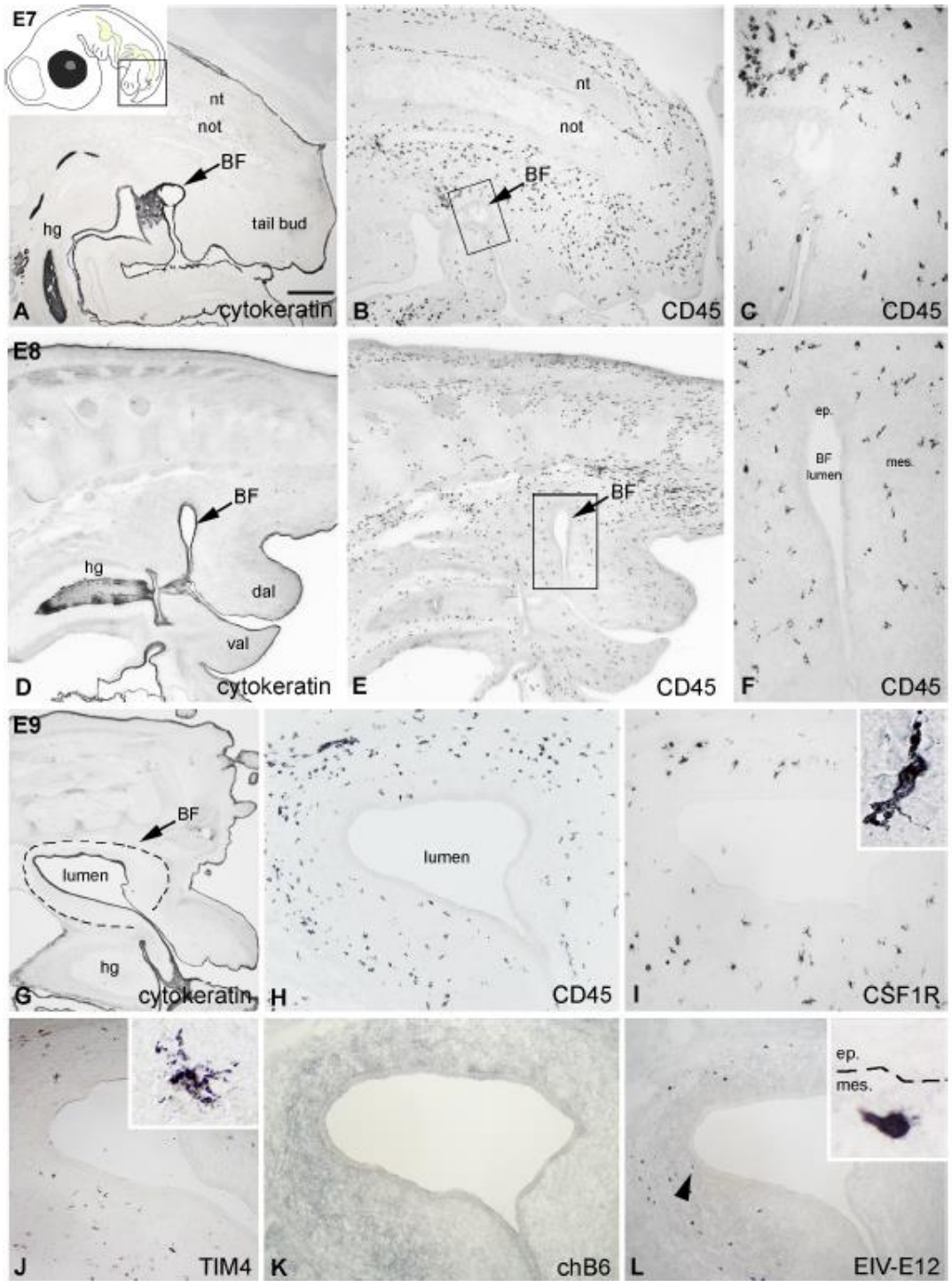


Figure 3. Hematopoietic colonization of the bursa of Fabricius. (A) E7: Initiation of the cytokeratin+ epithelial anlage, which remains continuous with the proctodeal region of the cloaca (arrow). **(B)** CD45+ hematopoietic cells are scattered in the tail bud and cloacal mesenchyme. **(C)** High magnification of the boxed area in B. **(D-F) E8:** CD45+ cells infiltrate the bursal mesenchyme, migrate close to the cytokeratin+ surface epithelium. Boxed

area magnified in F. **(G) At stage E9:** The bursal lumen expands and is delineated by the cytokeratin+ epithelium. The outlined area indicates the BF (arrow). **(H)** Immigrating CD45+ hematopoietic cells colonize the mesenchyme adjacent to the surface epithelium. **(I, J)** The outer mesenchymal region contains two distinct myeloid cell populations marked by the expression of CSF1R- and TIM4-specific mAbs. **(K)** chB6+ B cell precursors are absent from the bursa mesenchyme. **(L)** The EIV-E12 mAb labels a subpopulation of colonizing lymphoid cells. nt, neural tube; not, notochord; hg, hindgut; BF, bursa of Fabricius; dal, dorsal anal lip; val, ventral anal lip; ep, epithelium; mes, mesenchyme. Arrows indicate the bursal primordium. Scale bar: 400 μm **(A, B)**, 150 μm **(C)**, 400 μm **(D, E)**, 170 μm **(F)**, 300 μm **(G)**, 120 μm **(H-L)**, 20 μm [**(I, J)** insets], 12 μm [**(L)** inset]. (Szőcs et al., 2024)

4.1.2. CD45+/EIV-E12+ cells colonize the bursal epithelium

Infiltration of the bursal surface epithelium by blood-borne CD45+ cells can be first observed at E10 (Fig. 4A, B). Previous histology studies using toluidine-blue-stained semithin sections and TEM reported that the first cell population colonizing the bursal epithelium shows a basophilic, “dark” staining. It was suggested that this initial interaction results in the formation of dendro-epithelial follicle buds visible by E11 (Lupetti et al., 1990; Nagy et al., 2004b; Oláh et al., 1986). These cells were often identified as dendritic cell precursors, which form a transient dendro-epithelial structure to receive B cell precursors (Nagy et al., 2004a; Oláh and Nagy, 2013). To characterize these epithelium-infiltrating cells, mid-sagittal sections of E10 chicken embryo tail-bud were stained with lymphoid- and myeloid-specific antibodies. At this developmental stage CSF1R+ myeloid cells are uniformly scattered in the bursa mesenchyme (Fig. 4C), while chB6+ B cells are very few in number and are restricted to outer mesenchymal regions (Fig.4D). In contrast, the EIV-E12 monoclonal antibody consistently labels cell clusters localized within the surface epithelium (Fig. 4E). Immunolabeling on semithin and ultrathin sections confirms the basophilic, “dark” cell specificity of the EIV-E12 antigen (Fig. 4F, inset). Of note, EIV-E12+ cells often exhibit a single, spike-like process that points towards the surface epithelium (Fig. 4F, G).

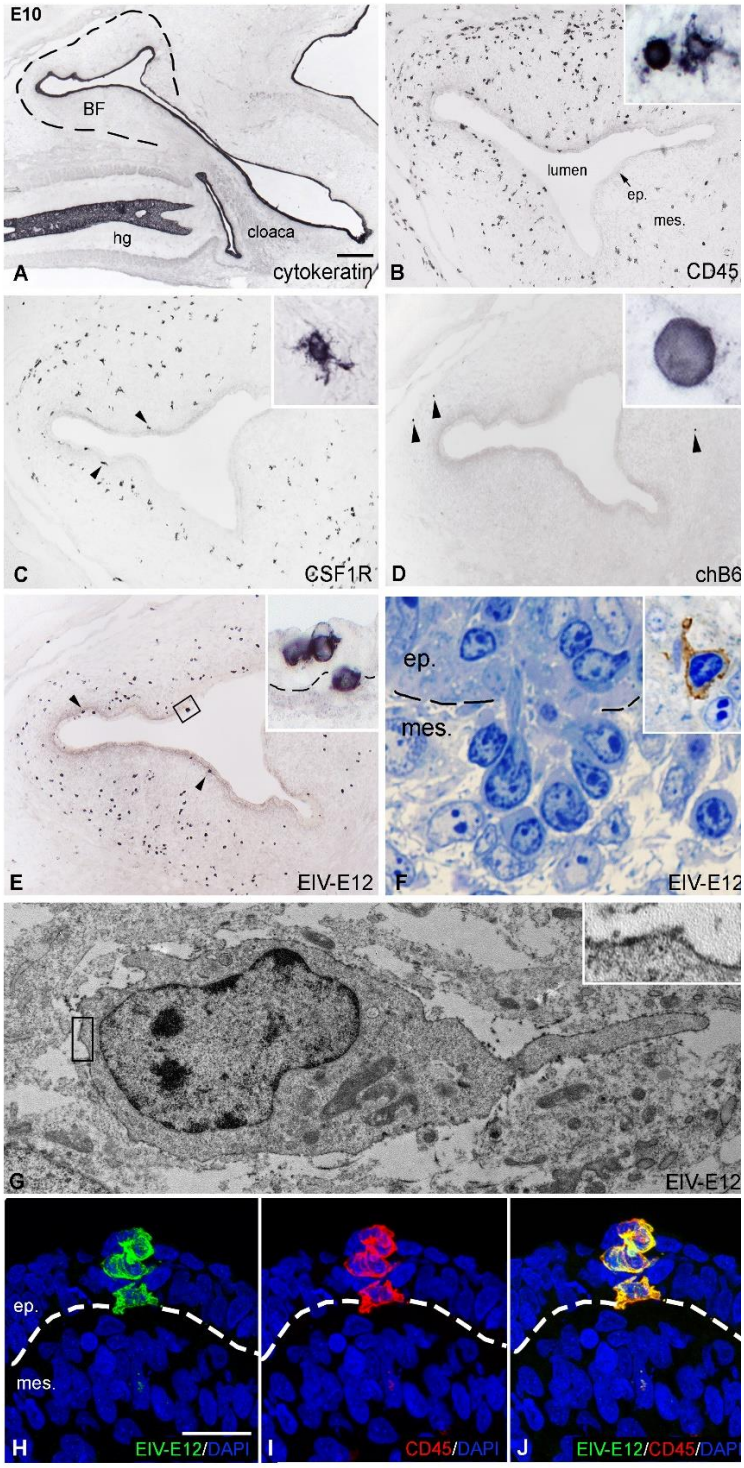


Figure. 2. Initiation of follicle bud formation. (A) The cytokeratin+ epithelial anlage of the E10 BF is a vesicle-like structure (dashed line) surrounded by the tail bud mesenchyme. **(B)** CD45+ hematopoietic cells (inset) are present in large numbers in the bursal mesenchyme and some of the cells reach the surface epithelium (arrow). **(C)** CSF1R+ ramified cells are localized in the bursal mesenchyme, a few cells present under the surface epithelium (arrowheads). **(D)** Presence of chB6+ B cell precursors in the bursal rudiment can be first observed on E10 in the peripheral mesenchyme (arrowheads). **(E)** Many EIV-E12+ cells are grouped under the surface epithelium (arrowheads), cross the basement membrane and induce the formation of follicle buds. Outlined area is magnified in inset. **(F)** Toluidine blue stained 1 µm thin section of a group of darkly stained cells crossing the basement membrane of the surface epithelium. Dashed line marks the BM. Inset: EIV-E12 immunohistochemistry on semithin section. **(G)** Immunoelectron microscopy of EIV-E12+ cell shows a poorly developed cytoplasm with few organelles, euchromatic nucleus and a single cellular process. Brown chromogen outlined in inset, marks the EIV-E12 immunoreactivity. **(H-J)** Groups of round EIV-E12+ cells co-express the common leukocyte antigen (CD45) and cluster inside the surface epithelium. ep, epithelium; mes, mesenchyme; hg, hindgut; BF, bursa of Fabricius. Scale bar: 300 µm (A), 120 µm (B, C, D, E), 10 µm (B inset), 14 µm (C inset), 5 µm (D inset), 8 µm (E inset), 4 µm (F), 5 µm (F inset), 800 nm (G), 180 nm (G inset).

4.1.3. Follicle bud formation coincides with the colonization of EIV-E12+/*CSF1R*-eGFP- cells to the epithelium

Transgenic reporter models are powerful tools for distinguishing cells of the macrophage lineage. The *CSF1R*-eGFP transgenic chicken line was created to visualize myeloid cells committed to the macrophage or dendritic cell lineage (Balic et al., 2014). To exclude the myeloid origin of colonizing EIV-E12+ cells, we analyzed the formation of follicle buds in *CSF1R*-eGFP embryos between E10-13. At E10, the *CSF1R*-eGFP transgene is present in ramified cells of the tail bud, hindgut, and bursal mesenchyme (Fig.5A). Immunostaining for CD45 shows the presence of two distinct populations that can be segregated based on their *CSF1R*-eGFP expression. CD45+/*CSF1R*-eGFP- cells reach the surface epithelium at E10, while a population of CD45+/*CSF1R*-eGFP+ ramified cells is present in the mesenchyme adjacent to the epithelium (Fig.5B). EIV-E12 immunostaining confirms that *CSF1R*-eGFP- cells that colonize the surface epithelium express the EIV-E12 antigen (Fig.5C, D). Several clusters of CD45+/EIV-E12+/*CSF1R*-eGFP- cells can be detected at the level of the surface epithelium by E11. The appearance of EIV-E12+/*CSF1R*-eGFP- cells in the epithelium always precedes *CSF1R*-eGFP+ ramified cell colonization. To further characterize the immigrating myeloid cells that belong to the *CSF1R*-eGFP lineage, we performed immunostaining for the TIM4 receptor, suitable for detecting mammalian and avian macrophages. Immunofluorescence shows a subpopulation of *CSF1R*-eGFP+ cells that co-express the TIM4 antigen. Both CSF1R+/TIM4+ and CSF1R+/TIM4- populations are present at the level of the developing follicle buds and the surrounding mesenchyme, bordered by the agrin+ basement membrane that runs between the prospective follicular medulla and cortex (Fig. 5J-L). chB6+ B cells can be first detected within the developing follicle buds at E13 (Fig.5M).

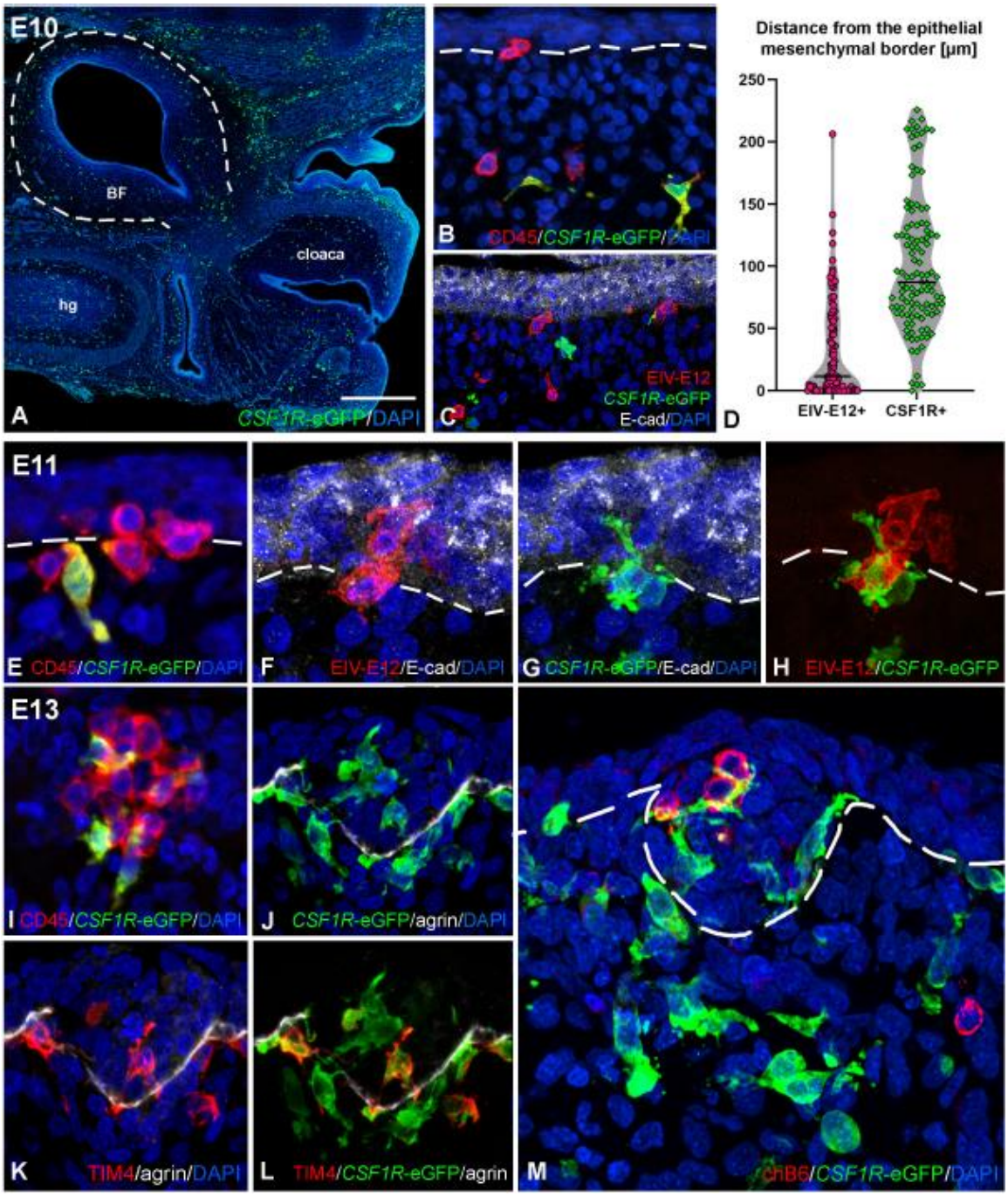


Figure 5. Folliculogenesis in *CSF1R*-eGFP transgenic chicken embryos. (A) Median-sagittal sections of E10 embryo tail bud show *CSF1R*-eGFP+ cells scattered in the BF mesenchyme. The outlined area marks the BF. **(B)** CD45+/*CSF1R*-eGFP- cells of round morphology reach the bursal surface epithelium, whereas CD45+/*CSF1R*-eGFP+ cells of ramified morphology are restricted to the bursal mesenchyme. **(C)** EIV-E12+ cells colonize the E-cadherin+ surface epithelium. EIV-E12+ cells do not express *CSF1R*-eGFP. **(D)** Quantification of the distance (µm) of colonizing EIV-E12+ and *CSF1R*-eGFP+ cells from

the surface epithelium. **(E-H)** Consecutive sections of E11 *CSF1R*-eGFP BF: epithelial colonization by EIV-E12+ cells is followed by the entry of *CSF1R*-eGFP expressing cells. **(I)** At E13, the follicle buds contain CD45+ cells of both round and ramified morphology. **(J-L)** Two distinct ramified cell populations can be distinguished inside the forming follicles: *CSF1R*-eGFP+/TIM4- dendritic cell precursors and *CSF1R*-eGFP+/TIM4+ macrophage precursors. **(M)** chB6+ B cells first colonize the follicle buds on E13. Dashed lines mark the epithelial basement membrane in (B, E-H, M). hg, hindgut; BF, bursa of Fabricius. Scale bar: 340 µm (A), 30 µm (B, C), 15 µm (E-H, M), 20 µm (I-L). (Szőcs et al., 2024)

4.1.4. EIV-E12+ cells do not give rise to dendritic cells or B cells

It has been suggested that EIV-E12+ cells represent a progenitor population for CSF1R+ bursal secretory dendritic cells (Pharr et al., 1995b). This hypothesis was also supported by observations made in chemically bursectomized birds, where testosterone-propionate treatment led to the absence of bursal secretory dendritic cells (BSDCs), inhibiting follicle formation and consequently the development of a functional bursa (Nagy and Oláh, 2009; Oláh et al., 1986). However, the direct link between EIV-E12+ early bursal cells and secretory dendritic cells has never been established. Moreover, during later maturation stages, B cells uniformly express the EIV-E12 antigen (Felfoldi et al., 2015; Pharr et al., 1995b), which raises the possibility that EIV-E12+ cells in the early bursal rudiment may represent a progenitor population for B cells.

To investigate the differentiation potential of the early colonizing EIV-E12+ cells, we performed a chick-duck chimera. This embryo manipulation method allows to fate map EIV-E12+ cells within developing bursal follicles. Antibodies used for the detection of colonizing lymphoid and myeloid populations were previously tested for species cross-reactivity, confirming that EIV-E12, TIM4, CSF1R, and B cell-specific chB6 do not cross-react with duck tissue (data not shown). For the identification of duck leukocytes, the anti-duck CD8 mAb was used. The specificity of this mAb to bursal B lymphocytes has been previously validated (Kothlow et al., 2005).

Chicken BF rudiments were harvested at E9, a stage when EIV-E12+ cells have already colonized the bursa mesenchyme but have yet to infiltrate the epithelium. Grafts were subsequently transplanted on the chorioallantoic membrane (CAM) of E11 duck embryos, which supports the development of the transplanted bursal rudiment through the richly

vascularized CAM (Fig. 6A-A"). Grafts were allowed to develop *in ovo* for 7 and 11 days and processed for immunohistochemistry.

After 7 days of incubation, bursal grafts exhibited the characteristic development of mesenchymal folds bulging into the bursal lumen (Fig.6B). Bursal folds are lined by the surface epithelium positive for BEN (Fig. 6C), an immunoglobulin superfamily molecule expressed on the surface of neurons and the epithelium of the BF (Pourquié et al., 1990). EIV-E12 immunolabeling confirms that cells have successfully colonized the surface epithelium in a pattern characteristic of normal embryonic development (Fig. 6D, inset). After 11 days of incubation, the grafts display several well-differentiated follicles. Immunolabeling with the chicken cell-specific mAb, 8F3, confirmed that both the mesenchymal and epithelial compartments were of chicken origin (Fig. 6E, F). Notably, the developing follicles were colonized by duck-derived CD8+ leukocytes (Fig. 6E inset). While initially EIV-E12+ cells were clustered within the surface epithelium at the level of the developing follicle buds, they were later restricted to the interfollicular connective tissue and the follicular medulla (Fig. 6E, inset). The chimeric follicles lacked donor chicken embryo-derived 8F3+/CSF1R+ myeloid and 8F3+/chB6+ lymphoid cells (data not shown), confirming that leukocyte populations were recruited from the host (duck), rather than differentiating from EIV-E12+ cells already present in the graft at the time of transplantation.

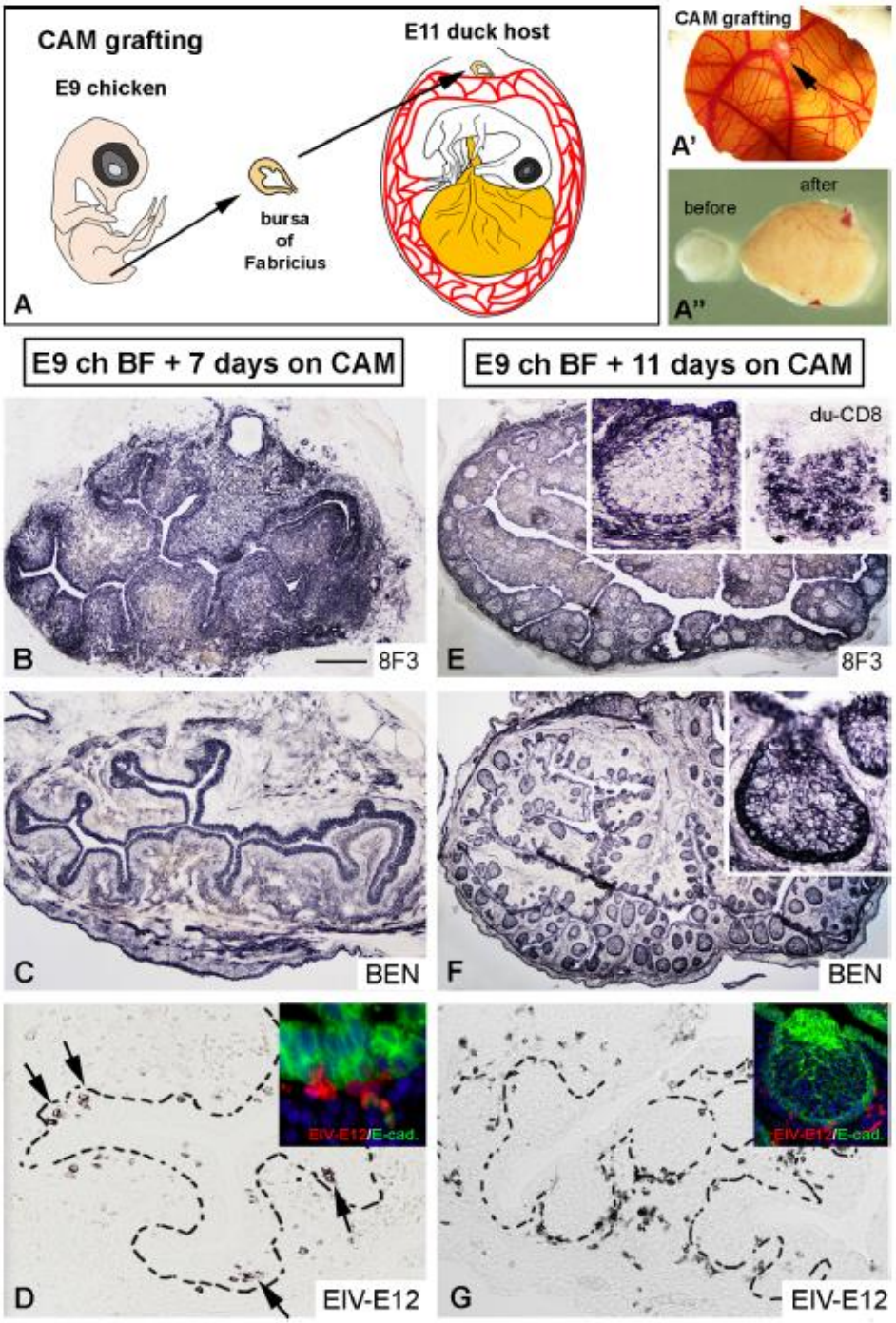


Figure 6. Duck-chicken chorioallantoic membrane transplantation reveals that EIV-E12+ cells are not precursors for dendritic cells or B cells. (A) To fate map the EIV-E12+ cells in the developing bursal follicles, E9 chicken bursa of Fabricius were cultured for up to 11 days on E11 duck CAM (n=8). **(A')** Chicken bursa graft on the CAM after 11 days of incubation (arrow). **(A")** Comparison of bursal size before and after chorioallantoic membrane transplantation. **(B)** 8F3 chicken cell-specific mAb marks the developing

epithelial-mesenchymal rudiment of the bursa. **(C)** Bursal epithelium shows BEN immunoreactivity. **(D)** Consecutive section shows EIV-E12 immunoreactive cells colonizing the surface epithelium (arrows). Example of EIV-E12+ cells entering the E-cadherin+ surface epithelium shown in inset. **(E, F)** 11 days after CAM transplantation, the BF develops several folds, filled with lymphoid follicles, which are colonized by CD8+ leukocytes of duck origin (inset Figure 4E). **(G)** Few EIV-E12+ cells are present at the margin of the follicles, and many are excluded to the interfollicular space. Scale bar: 6 mm (A'), 1 mm (A"), 250 µm (B, C), 50 µm (D), 30 µm [(D) inset], 350 µm (E, F), 150 µm (G), 70 µm [(E–G) inset] (Szőcs et al., 2024).

4.1.5. Follicle bud induction occurs independently of dendritic cell and B cell precursors

The classical model for bursal hematopoietic colonization is primarily based on quail-chick chimeric studies, in which sequential colonization starts with the infiltration of the epithelium by 74.3+ dendritic cell precursors (Nagy et al., 2004a; Oláh and Nagy, 2013; Yvernogeau et al., 2022). The formation of this dendro-epithelial tissue is considered a prerequisite of B cell colonization of bursal follicles. It has previously been shown that this sequential colonization is highly sensitive to hormonal treatment by testosterone propionate and results in chemical bursectomy by arresting the differentiation of 74.3+ dendritic cells, which subsequently leads to the failure of normal BF development (Nagy and Oláh, 2009; Oláh et al., 1986; Wilson and Boyd, 1990).

To investigate the initial steps of follicle bud formation in the absence of dendritic cells, we performed chemical bursectomy (Fig. 7A) and analyzed bursal follicle formation at E14. In control bursae, EIV-E12+ cells are grouped in the surface epithelium at the level of the follicle buds (Fig. 7B, C), which are colonized by dendritic cells (Fig. 7D) and B cells (Fig. 7E). In this experiment, BSDCs were immunolabeled by the 74.3 monoclonal antibody, and B cells were detected by anti-chB6 (Igyártó et al., 2008; Soós et al., 2025). In contrast, dendritic cells are entirely absent in the TP-treated group (Fig. 7H), a phenomenon that does not affect epithelial follicle bud induction. EIV-E12+ cells are present in large numbers within the bursal folds, clustered at the level of the surface epithelium (Fig. 7F, G). While scattered chB6+ B cells can be found within the mesenchyme, the number of colonizing B cells is markedly reduced (Fig. 6I). These findings suggest that the initial steps of follicle bud formation are not dependent on the presence or differentiation of 74.3+ dendritic cells.

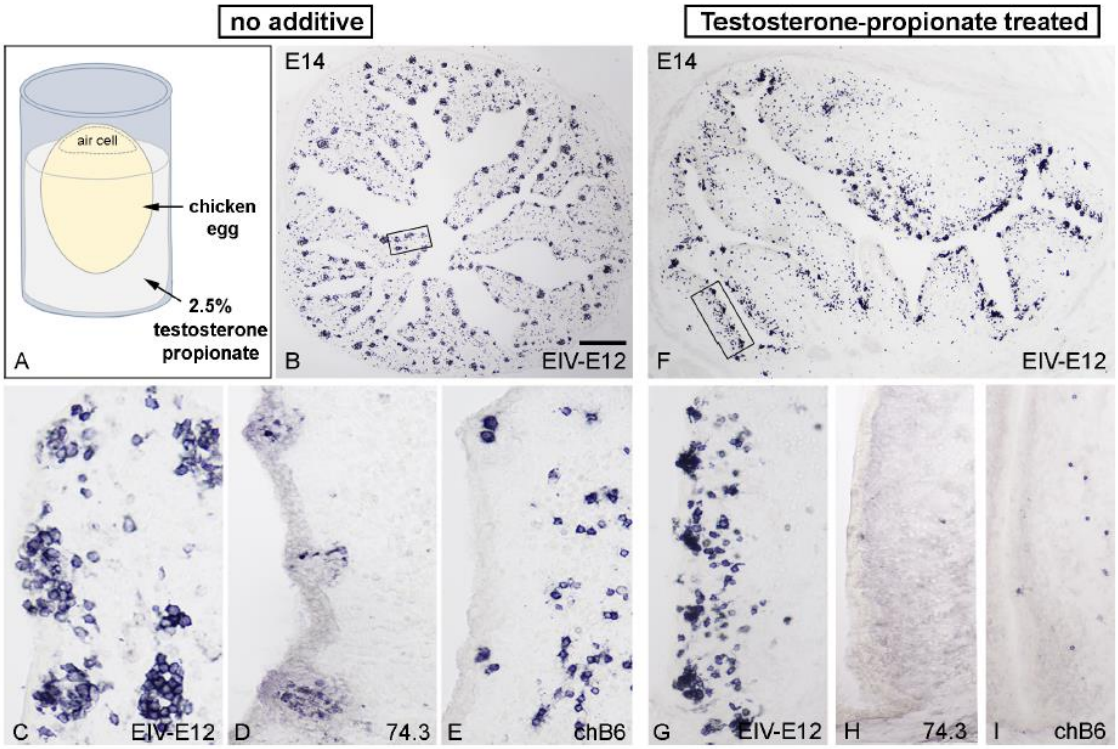


Figure 7. Testosterone-propionate treatment inhibits dendritic cell differentiation but does not influence follicle bud formation. (A) To test whether the absence of dendritic cells could affect follicle formation, one-day-old chicken eggs were treated with 2.5% testosterone propionate and further incubated until E14. **(B)** Control bursae show normal follicle development (n=8), with EIV-E12+ cells filling the epithelial buds along the bursal folds. Boxed area magnified in **(C)**. General view from E14 bursa showing the presence of EV-E12+ cells. **(D)** 74.3+ dendritic cells and **(E)** chB6+ B cells colonize the developing follicle buds. **(F)** Testosterone treatment does not inhibit EIV-E12+ cell colonization of the surface epithelium (n=8). Boxed area magnified in **(G)**. Compared with control bursae, EIV-E12+ follicle buds develop in large numbers along the axis of the folds. **(H)** In contrast, 74.3+ dendritic cells are absent in testosterone-treated bursae. **(I)** Few chB6+ B cells are present in the mesenchyme of the folds and occasionally migrate into the surface epithelium. Scale bar: 280 µm (B), 50 µm (C-E), 230 µm (F), 75 µm (G-I) (Szőcs et al., 2024).

To test whether the absence of B cells affects the initial steps of follicle bud formation, we used a recently described model, in which B cell depletion in the bursa of Fabricius was achieved by using the CXCR4 receptor antagonist AMD3100 (Nagy et al., 2020). E9 BF primordia were isolated and injected with AMD3100 or PBS (control) and were transplanted on the chorioallantoic membrane of E9 host chicken embryos, which were further incubated for 9 days. In control bursa grafts, well-developed chB6+ lymphoid follicles fill the bursal

folds (Fig. 8A). The BEN+ epithelial follicles contain chB6+ B cells that co-express the EIV-E12 antigen (Fig. 8B-D) and dendritic cells expressing the 74.3 antigen (Fig. 8E). While in E9 bursal grafts treated with AMD3100 the number of chB6+ cells was markedly reduced, the absence of B cells did not affect lymphoid follicle formation. Both 74.3+ dendritic cells and EIV-E12+ cells colonized the bursal surface epithelium. These results demonstrate that the initial steps of follicle formation do not rely on signals or cell-cell interactions from migrating BSDCs or B cell precursors.

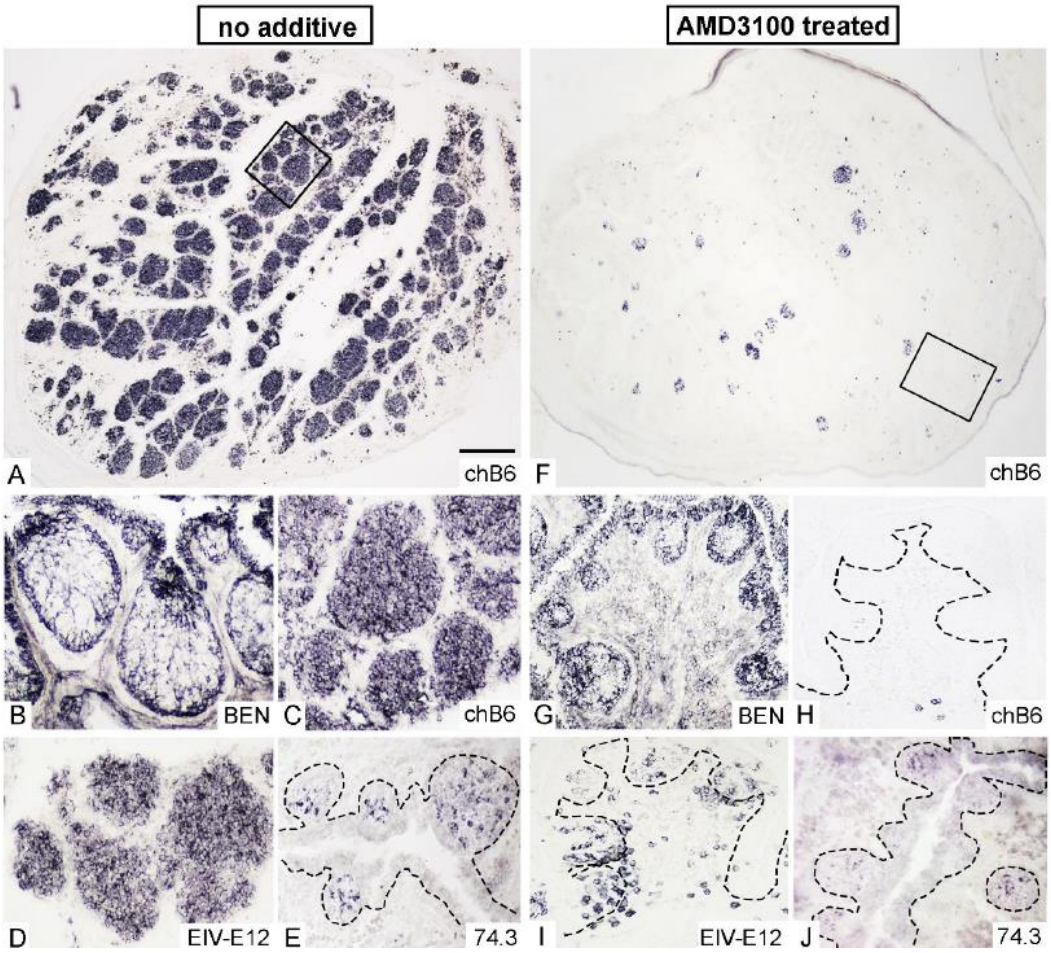


Figure 8. Depletion of B cells does not prevent follicle bud formation. E9 bursa of Fabricius was injected with the CXCR4 inhibitor AMD3100 (n=9) or vehicle (no additive, n=6) and cultured on the chorioallantoic membrane (CAM) of E9 host chick embryo. **(A)** Non-treated bursa of Fabricius shows a well-developed lymphoid follicular structure. **(B, C)** BEN+ epithelial follicles are filled with chB6+ B cells. **(D)** Distribution of EIV-E12+ cells corresponds to B-dependent follicles. **(E)** 74.3+ dendritic cells are observed in the follicles. **(F)** Addition of AMD3100 inhibits B cell colonization of the bursa of Fabricius. Boxed area in F is shown in H. **(G)** BEN immunoreactivity labels the bursal epithelium with growing

epithelial buds towards the mesenchyme. **(I)** EIV-E12+ cells are present in large numbers in the epithelial follicle buds. **(J)** AMD3100 treatment did not influence the colonization of 74.3+ dendritic cells in the bursa follicles. Scale bar: 280 µm (A), 80 µm (B-E), 220 µm (F), 50 µm (G-J) (Szőcs et al., 2024).

4.1.6. EIV-E12+ cells induce follicle bud formation

To confirm the inductive role of EIV-E12+ cells, quail-chick epithelial-mesenchymal recombination experiments were performed (Nagy and Oláh, 2010; Nagy et al., 2016b). E8 quail BF epithelium was enzymatically digested from the associated mesenchyme and recombined with either E9 chicken BF mesenchyme (Experiment 1) or E9 chicken hindgut mesenchyme (Experiment 2). Recombinants were allowed to develop on the surface of a collagen gel matrix for 24 hours to ensure tissue adherence before being transplanted onto the chorioallantoic membrane of E9 chicken host embryos. The CAM chimeras were allowed to develop for an additional 9 days (Fig. 9A).

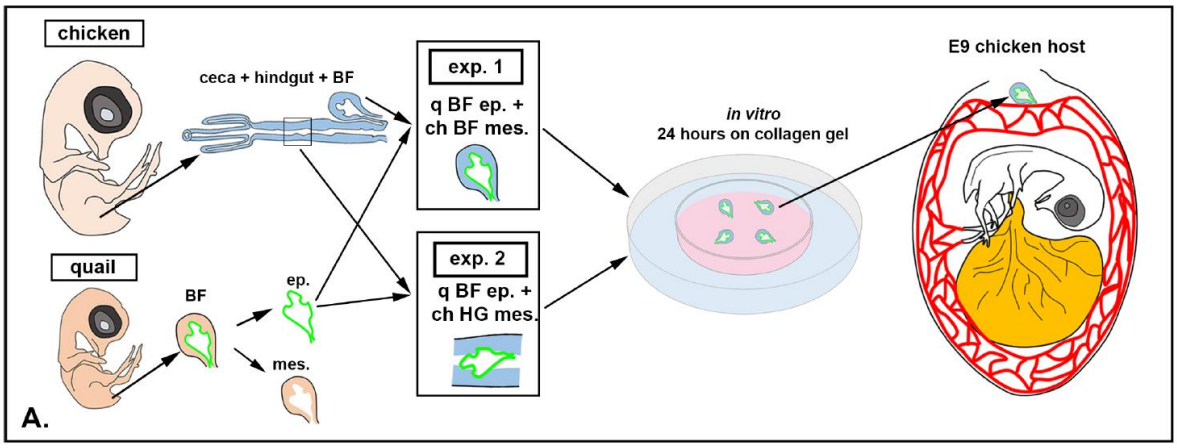


Figure 9. Schematic illustration of quail-chick epithelial-mesenchymal recombination.

In Experiment 1, where quail BF epithelium was recombined with chicken BF mesenchyme, the chimeric graft showed normal folliculogenesis, characterized by the successful recruitment of chicken embryo-derived chB6+ B cells, CSF1R+ dendritic cells, and TIM4+ macrophages into the quail-derived epithelial follicles, confirmed by QCPN positivity (Fig. 10B-F). In contrast, when quail BF epithelium was recombined with chicken hindgut mesenchyme (Experiment 2), which does not harbor EIV-E12+ cells (data not shown), the grafts failed to develop follicle buds (Fig. 8G). Although host CD45+

hematopoietic cells infiltrate the hindgut mesenchyme, the absence of EIV-E12+ cells from the hindgut mesenchyme prevents the differentiation of lympho-epithelial follicle buds from the quail-derived BF epithelium (Fig. 8H, I). These findings demonstrate that EIV-E12+ cells are essential drivers of follicle bud initiation within the bursal microenvironment.

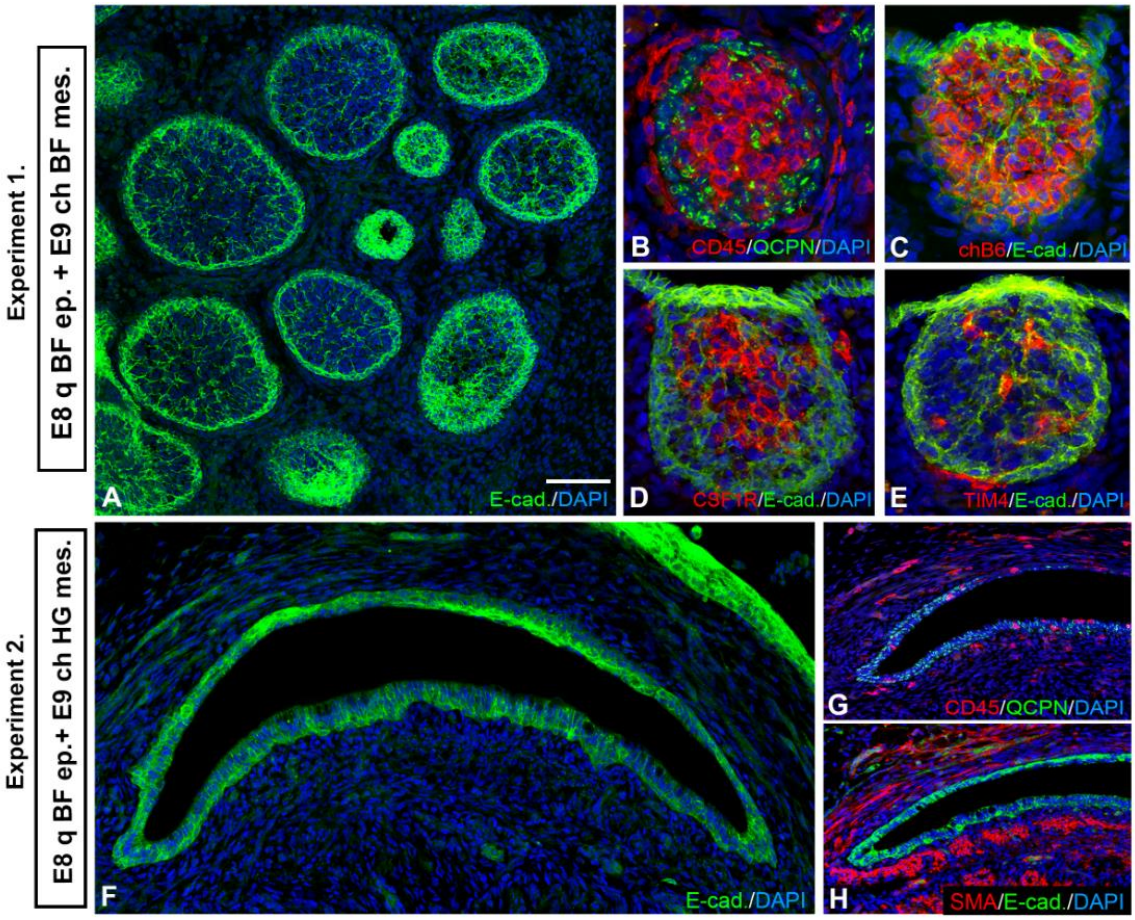


Figure 10. EIV-E12+ cells induce follicle bud formation. (A) In Experiment 1 (n=5), where quail BF epithelium was recombined with chicken BF mesenchyme, normal follicle development was observed. **(B)** CD45+ hematopoietic cells colonize the developing follicles. QCPN immunostaining confirms that the epithelium is quail-derived. **(C-E)** Each follicle contains chB6+ B cells (C), CSF1R+ dendritic cells (D), and TIM4+ macrophages (E). **(F-H)** In Experiment 2 (n=5), where quail hindgut epithelium was recombined with bursa mesenchyme, no lymphoid follicles formed. **(F)** E-cadherin immunostaining reveals the differentiation of the epithelium. **(G)** QCPN immunostaining confirms that the epithelium is quail-derived. CD45+ cells colonize the grafts, but cell clustering or follicle formation is not observed. **(H)** Staining for alpha-smooth muscle actin (SMA) showed a muscularis layer located immediately under the epithelium. q, quail; ch, chicken; ep, epithelium; mes, mesenchyme; BF, bursa of Fabricius; HG, hindgut. Scale bar: 180 µm (A-E), 350 µm (F-H).

4.2. Development of the lymphoid follicular cortex and mechanisms of cortical B cell emigration

4.2.1. Characterization of lymphoid follicles in the chicken bursa of Fabricius

During embryonic development, expansion and maturation of B cells occur within the specialized microenvironment of bursal follicles, which show a compartmentalization that first becomes apparent post-hatch. Follicles have a central loosely packed medulla and a peripheral, highly dense cortex (Fig. 11A), both of which have individual myeloid and stromal cell populations. While the lympho-myeloid and stromal components of the medulla have been extensively characterized (Balic et al., 2019; Fejszák et al., 2022; Nagy et al., 2004a; Nagy et al., 2016a; Nagy et al., 2022; Oláh et al., 1986), the development, cellular, and molecular microenvironment of the cortex remains largely underexplored. Ultra-structural characterization by electron microscopy reveals that, similar to the medulla, the most abundant cell type in the cortex is B cells, which are localized between a 3D network of cortical reticular cells (Olah et al., 2022). Reticular cells are morphologically distinct, characterized by euchromatic nuclei and several cellular processes (Fig. 11B, C).

While adult lymphoid follicles represent a functional unit, the medulla and the cortex have distinct origins, resulting in different stromal scaffolds for resident B cell populations (Nagy and Oláh, 2010; Nagy et al., 2004a). The reticular epithelial cells of the medulla develop from the ectoderm of the cloacal epithelium and express cytokeratin intermediate filaments (Fig. 11D). Unlike the medulla, the cortex is of mesodermal origin. Mesenchymal reticular cells in the cortex co-express vimentin and desmin intermediate filaments. RNAscope *in situ* hybridization further shows that the cortex is defined by a unique pattern of chemokine expression. Vimentin+ cortical reticular cells co-express the CXCL12 chemokine (Fig. 11F, inset). It has previously been described that cortical B cells selectively express the CXCR4 receptor (Laparidou et al., 2020; Nagy et al., 2020). *In situ* hybridization on consecutive sections demonstrates that $CXCR4^{high}$ B cells are restricted to the outer regions of the cortex, while $CXCR4^{low/dim}$ B cells are concentrated around the cortico-medullary border marked by the laminin+ basement membrane (Fig. 11G).

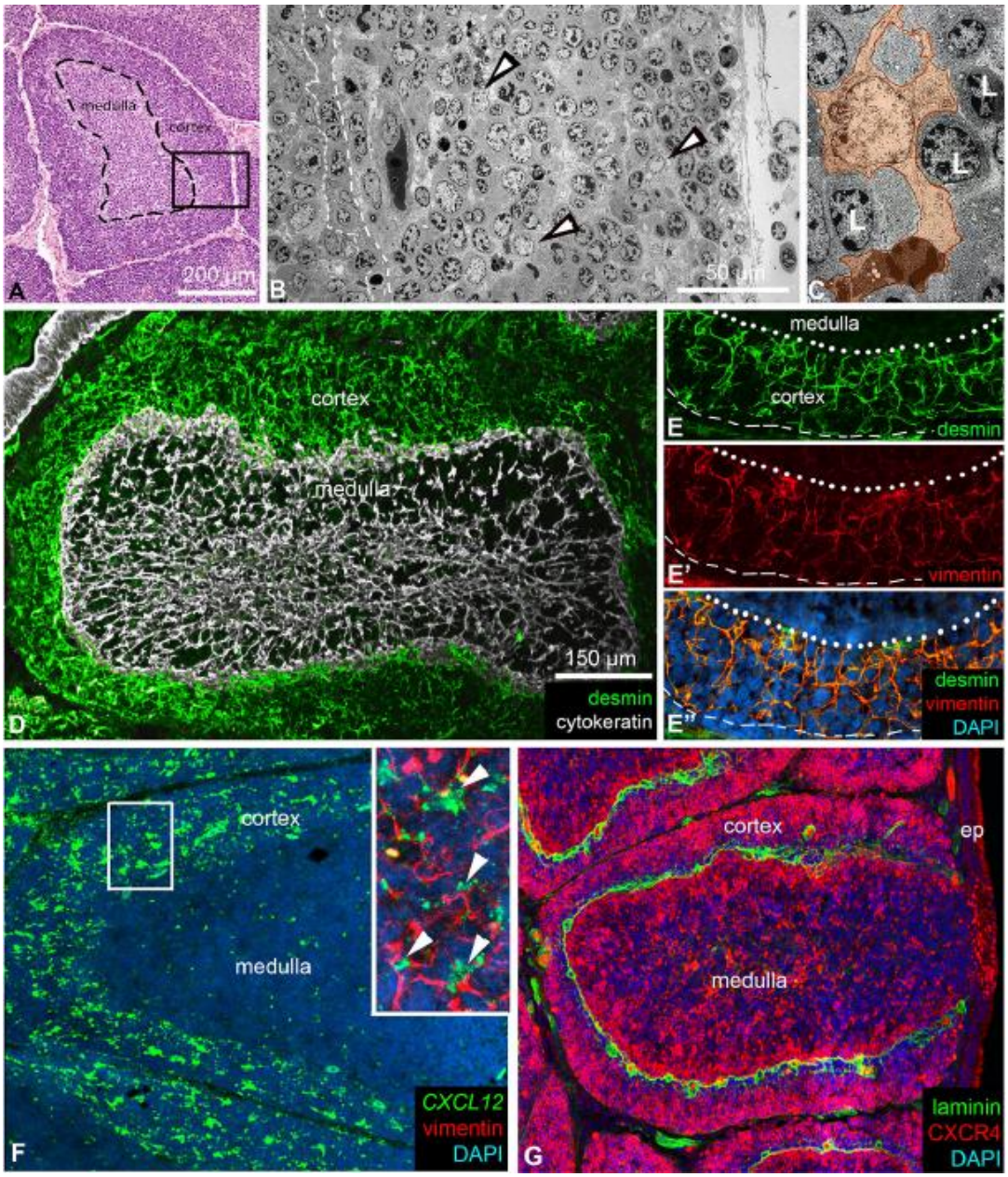


Figure 11. Structure of lymphoid follicles in the chicken bursa of Fabricius. (A) Hematoxylin-eosin-stained paraffin-embedded section of an 8-week-old chicken bursa of Fabricius. Each bursal follicle contains a central medullary and an outer cortical region, separated by a basement membrane (dashed line). **(B)** Electron micrograph of the cortex (see the outlined area in **A)** shows several reticular cells (arrowheads) scattered among cortical B cells. The outlined area marks the cortico-medullary epithelium. **(C)** The euchromatic nuclear structure of reticular cells (orange) differs from the heterochromatic nuclear structure of lymphocytes. **(D)** Reticular cells of the medulla are of epithelial origin and express cytokeratin intermediate filaments. In contrast, reticular cells of the cortex are of mesenchymal origin and are desmin+. **(E, E', E")** The dotted line indicates the cortico-

medullary border; the dashed line marks the outer border of the cortex. Desmin+ mesenchymal reticular cells co-express vimentin intermediate filaments. **(F)** Desmin+/vimentin+ reticular cells in the cortex uniformly express the CXCL12 chemokine ligand, shown by *in situ* hybridization. Magnified view in the inset. Arrowheads show CXCL12+/vimentin+ cortical reticular cells. **(G)** B cells within the cortex are CXCR4+. Laminin marks the basement membrane under the cortico-medullary border and around cortical capillaries (Soós et al., 2025).

4.2.2. The cortex is rich in extracellular matrix proteins

To characterize the immunophenotype of the cortical region, we performed a detailed cytochemical analysis using a large panel of monoclonal antibodies specific for glycoproteins, proteoglycans, and collagens. Collagens (type I, III, IV, and VI) are the most abundant ECM in the bursa, localized within the interfollicular connective tissue septae and the basement membrane of the cortico-medullary epithelium. They also exhibit a fine reticular network at the level of the cortex (Fig. 12A-D). Heparan-sulfate proteoglycans, such as collagen 18, perlecan, and agrin, are strictly confined to the basement membranes (Fig. 12E-G), while versican, a chondroitin-sulfate proteoglycan, is expressed only in the interfollicular connective tissue (Fig. 12H). Consistent with its role in basement membrane formation, laminin expression is restricted to the basement membrane of the cortico-medullary epithelium and the cortical capillaries (Fig. 12I). Other glycoproteins, such as fibronectin and fibrillin, show a robust staining in the interfollicular connective tissue and form a complex reticular network spanning the entire cortex from the inner cortico-medullary border to the outer interfollicular border (Fig. 12J, K). Interestingly, among glycoproteins, tenascin-C exhibits a highly specialized and restricted expression pattern. Unlike other ECM proteins, it is absent from the interfollicular connective tissue, and it is restricted to the inner cortical region, forming a three-dimensional network around cortical capillaries (Fig. 12L).

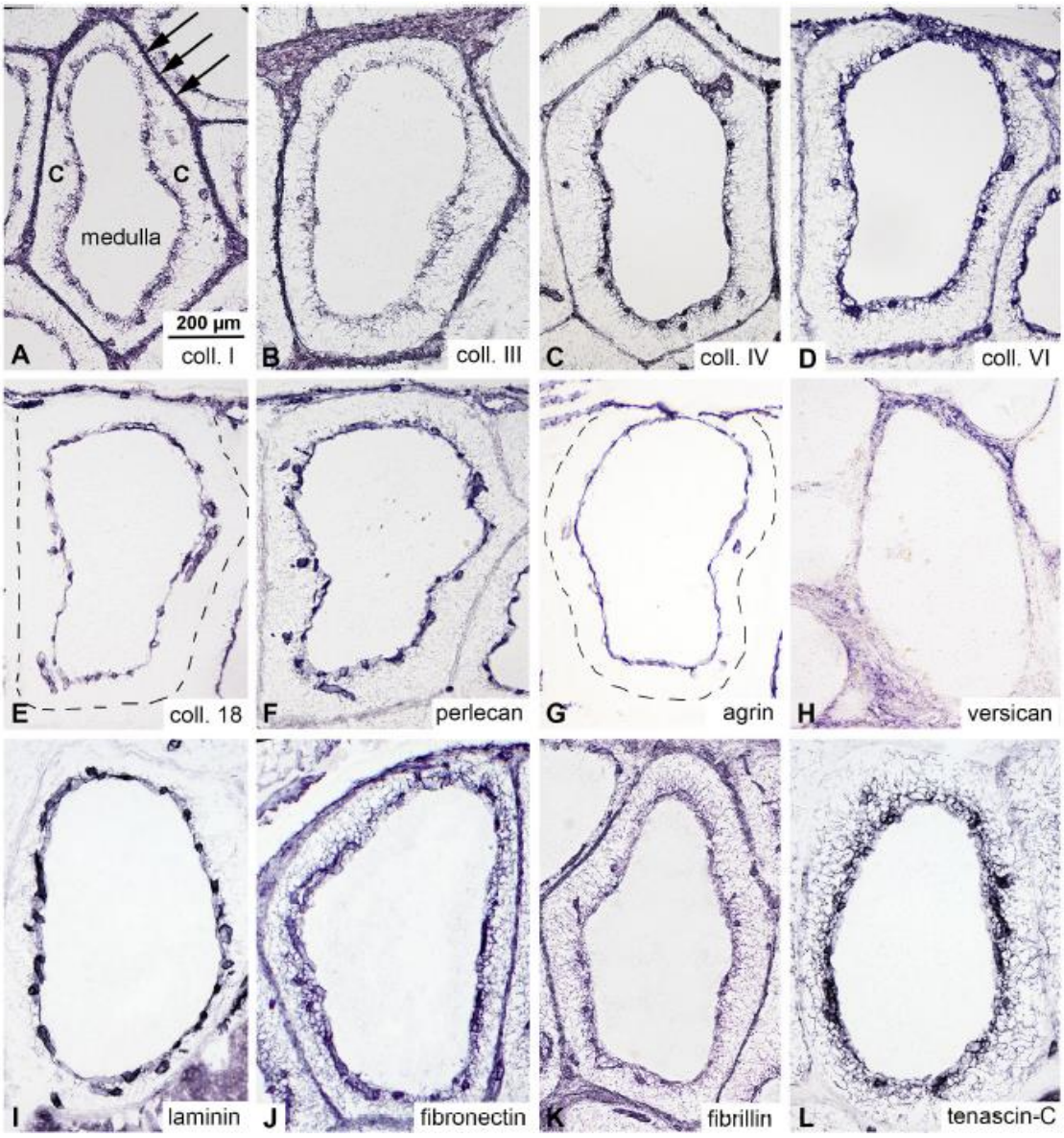


Figure 12. Expression of extracellular matrix proteins in the cortex of the bursal follicles. (A-D) Collagens are highly expressed in the cortex of the follicles and interfollicular connective tissue septum (arrows). There are no collagens inside the medulla. **(E-G)** Heparan-sulpate proteoglycans (collagen type 18, perlecan and agrin) are specifically expressed in the basement membrane of the cortico-medullary epithelium and cortical endothelial cells, respectively. **(H)** Versican, a chondroitin sulphate-type proteoglycan, shows concentrated interfollicular connective tissue immunoreactivity. Immunostaining of glycoproteins indicates that **(I)** laminin is specifically expressed in the basement membrane. **(J)** Fibronectin and **(K)** fibrillin are diffusely distributed throughout the cortex and interfollicular connective tissue, while **(L)** tenascin-C shows intense fibrillar staining concentrated in the inner region of the cortex (Soós et al., 2025).

4.2.3. Complementary expression of tenascin-C and CXCR4 in the follicular cortex

We have previously shown that the CXCR4 receptor selectively labels cortical B cells in adult lymphoid follicles (Nagy et al., 2020). When we compared the distribution of CXCR4 immunoreactive cells with the expression of tenascin-C, which is a cortex-specific ECM, we found that B cells with high CXCR4 expression are localized in outer cortical regions (Fig.13A). In contrast, B cells at the cortico-medullary border do not express the CXCR4 receptor ($CXCR4^{low/dim}$). When compared with the expression of tenascin-C, $CXCR4^{high}$ B cells are preferentially localized in cortical areas lacking tenascin-C. Within the inner region of the cortex, the localization of tenascin-C is not uniform: distinct gaps of low expression alternate with tenascin-C-rich perivascular zones (Fig. 13A inset, B). Similar to the segregation of $CXCR4^{high}$ and $CXCR4^{low/dim}$ cortical zones, we identified distinct cortical subpopulations based on their mitotic activity (Fig. 13C). $CXCR4^{high}$ cells are highly proliferative, while $CXCR4^{low/dim}$ cells constitute a quiescent cell population in the tenascin-C-rich inner cortex (Fig. 13D, E).

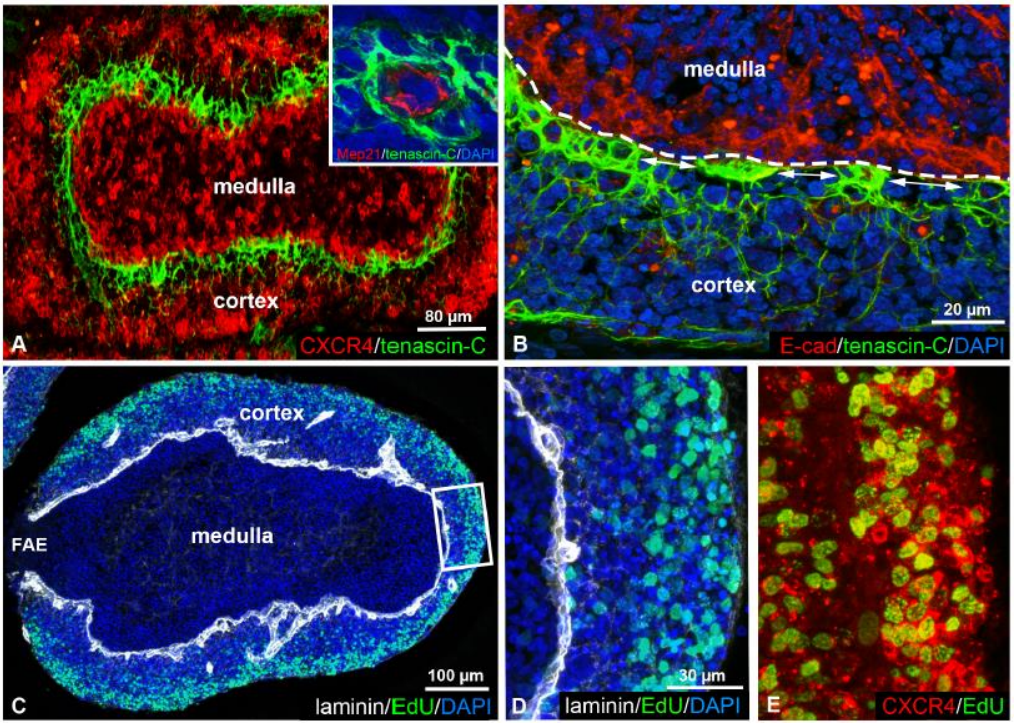


Figure 13. Tenascin-C and CXCR4 show a complementary expression pattern in the follicular cortex. (A, B) Double immunostaining of tenascin-C and CXCR4 in the adult

bursal follicle shows robust tenascin-C expression in CXCR4$^{low/dim}$ regions along the cortico-medullary border (dashed line). Tenascin-C immunoreactivity is highest around cortical capillaries (inset) at the E-cadherin+ cortico-medullary epithelium **(B)** and gradually decreases between the capillaries (double arrows) and towards outer cortical regions. **(C-E)** EdU incorporation reveals that CXCR4^{high} B cells in the outer cortex are highly proliferative. Laminin expression marks the basement membrane along the cortico-medullary border and around cortical capillaries (Soós et al., 2025).

4.2.4. Expression of tenascin-C in the embryonic bursa of Fabricius

To further characterize the spatiotemporal distribution of ECM molecules during bursal development and hematopoietic colonization, we compared the expression of tenascin-C with fibronectin. The earliest migratory wave of committed B cells reaches the bursa primordium at E11 of embryonic development. Comparative immunostainings confirm that all major ECM molecules, including glycoprotein, proteoglycan, and collagen type of proteins, are widely expressed within the BF mesenchyme (data not shown). Fibronectin acts as a key regulator of cell migration, facilitating cell movement, adhesion, and proliferation during BF embryonic development (Polajoki et al., 1993). Fibronectin is strongly expressed in the developing tail bud mesenchyme, hindgut mesenchyme and is ubiquitously present within the developing BF mesenchyme (Fig. 14A). In contrast, tenascin-C is absent from the bursal mesenchymal compartment during this initial period of active colonization (Fig. 14B). Expression of tenascin-C can be first detected at E13 in the connective tissue capsule of the developing BF (Fig. 14C). As development progresses, the ECM undergoes significant spatial reorganization. While the mesenchymal compartment of the bursal folds remains fibronectin positive, the emerging lympho-epithelial follicle buds do not express fibronectin (Fig. 14D). At this developmental stage, tenascin-C expression is localized within the mesenchymal compartment surrounding the larger lympho-epithelial follicles (Fig. 14E). This expression pattern is consistent with the emergence of the prospective cortical region, which further matures post-hatch. The appearance of tenascin-C within the perifollicular mesenchyme coincides with the loss of colonization potential of migrating B cell precursors (Nagy and Oláh, 2010).

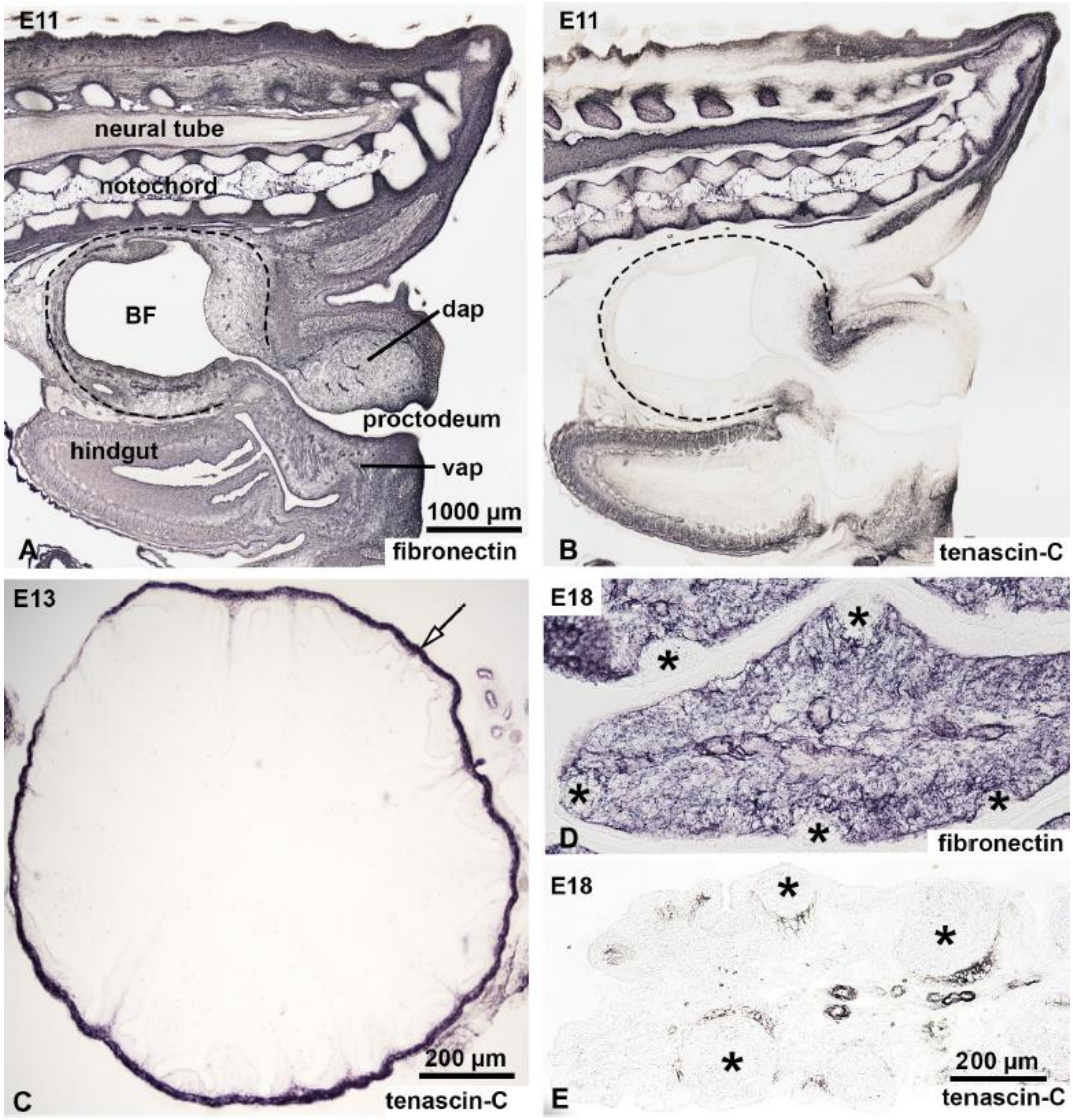


Figure 14. Expression of fibronectin and tenascin-C in the developing chick bursa of Fabricius. (A, B) Sagittal sections through the tail bud of an E11 embryo show the expression patterns of fibronectin and tenascin-C. Dashed lines mark the BF. **(A)** Anti-fibronectin immunostaining reveals robust expression in the extracellular matrix of the tail bud, the BF, and the hindgut mesenchyme. **(B)** Tenascin-C expression is restricted to the vertebral column, tip of the tail bud, and hindgut mesenchyme, with no detectable expression in the BF at this stage. **(C)** Transverse section of the BF at E13. Tenascin-C is absent in both the lymphoid compartment and the mesenchymal core of bursal folds. The connective tissue capsule of the BF (arrow) shows strong tenascin-C immunoreactivity. **(D, E)** Longitudinal section of the BF fold at E18. **(D)** Fibronectin is expressed uniformly in the mesenchymal compartment but is notably absent in the developing lymphoid follicles (asterisks). **(E)** Tenascin-C immunoreactivity emerges at E18 in the mesenchymal cells surrounding the developing follicles. BF, bursa of Fabricius; dap, dorsal anal lip; vap, ventral anal lip (Soós et al., 2025).

4.2.5. Shh-induced overexpression of tenascin-C disrupts lymphoid follicle formation

To assess the role of tenascin-C in the earliest stages of bursa development, we utilized the advantages of the avian embryo to experimentally manipulate the bursal mesenchymal environment. Sonic hedgehog (Shh) is not naturally expressed in the bursa of Fabricius at any point in development however, it is a known upstream regulator of tenascin-C expression. According to Ting-Berreth and Chuong (1996) retrovirus-mediated ectopic overexpression of Shh in the developing feather buds induces the robust expression of tenascin-C. Using the same Shh-replication-competent avian retrovirus (RCAS) (Riddle et al., 1993) we overexpressed Shh by injecting E9 BF primordia prior to hematopoietic colonization. The Shh-RCAS injected grafts were transplanted onto the chorioallantoic membrane of E9 host chicken CAM and further incubated for 8 days *in ovo* (Fig. 15A). CAM transplantation is a robust method that supports physiological development, which was confirmed by the formation of lymphoid follicles within the grafts, colonized by chB6+ B cells (Akbareian et al., 2013; Nagy et al., 2020). Control grafts showed robust development of the bursa primordium, with complete absence of the Shh protein (Fig.15B, C). Tenascin-C expression was exclusively found within the external connective tissue capsule of the bursa (Fig. 15D). In contrast, Shh-RCAS-injected grafts demonstrated robust viral infection throughout the mesenchyme, confirmed by anti-3C2 immunoreactivity specific for the gag protein of the RCAS viral capsid. This transduction resulted in high-level Shh protein expression (Fig. 15G) and subsequently in the upregulation of tenascin-C expression throughout the bursa mesenchyme (Fig. 15H). The presence of tenascin-C within the mesenchymal compartment resulted in impaired B cell colonization. In Shh-RCAS-injected grafts, the presence of chB6+ B cells is significantly reduced, resulting in the formation of only a few, rudimentary lymphoid follicles (Fig. 15I). In summary, the presence of tenascin-C during bursa colonization inhibits B cell colonization, suggesting that the exclusion of tenascin-C from the cloacal mesenchyme is required for lymphoid follicle colonization.

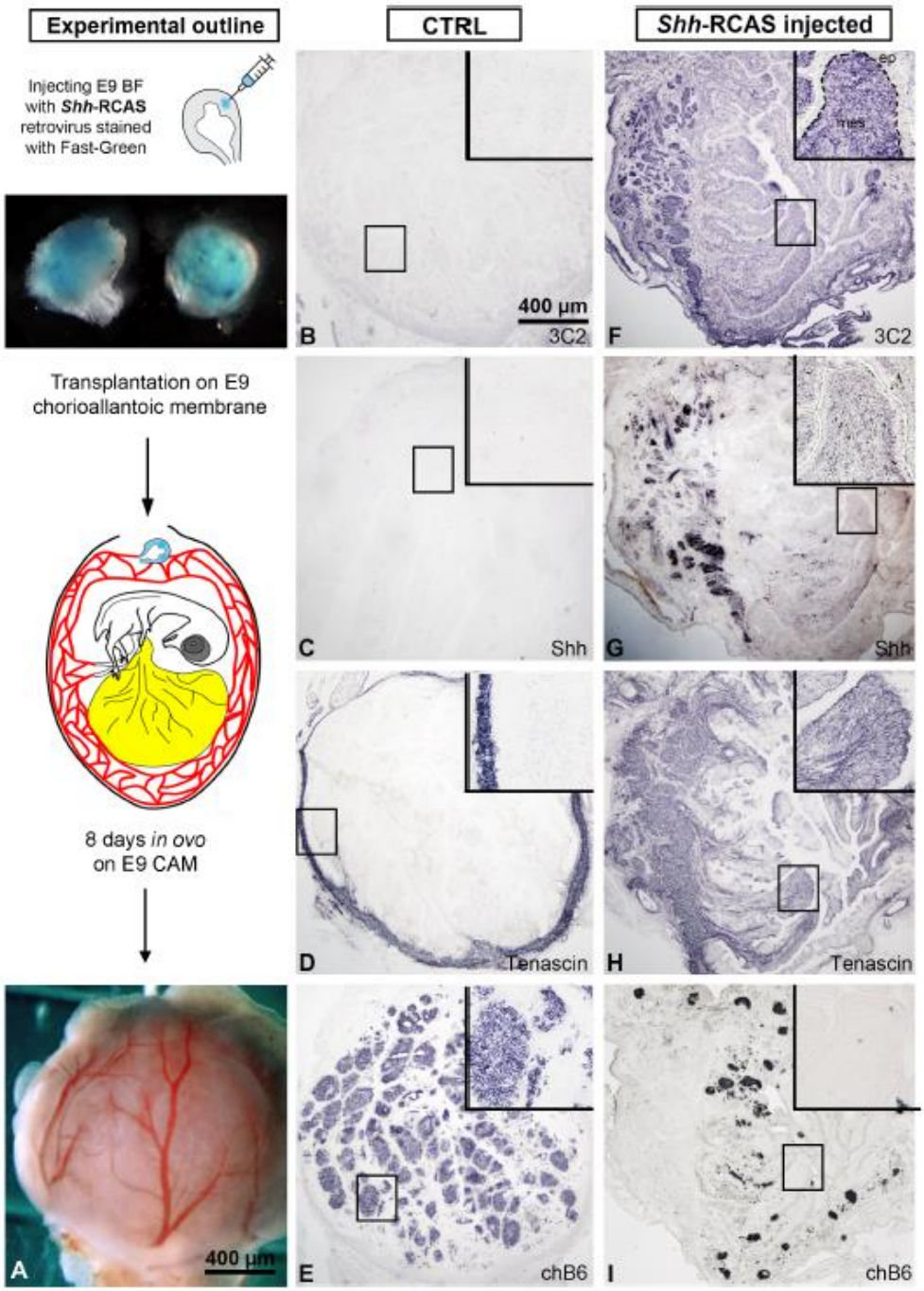


Figure 15. RCAS virus-mediated overexpression of Shh induces ectopic tenascin-C expression in the embryonic bursa mesenchyme. **(A)** Schematic illustration of the experimental setup, where dissected E9 bursa of Fabricius was injected *ex vivo* with RCAS-Shh and cultured *in ovo* for 8 days on an E9 chick chorioallantoic membrane (CAM). Magnified views of outlined bursal folds are shown in insets. Serial cross-sections from control CAM grafts were immunostained for the RCAS virus-specific 3C2 antibody **(B)**, Shh **(C)**, tenascin-C **(D)**, and chB6 **(E)**. **(F)** In *Shh*-RCAS-injected grafts, robust RCAS

expression was detected throughout the bursa mesenchyme using the 3C2 antibody, indicating effective viral transduction and ectopic Shh protein expression. **(G)** Shh expression was localized to the bursa mesenchyme, confirming successful overexpression. **(H)** Shh significantly upregulated tenascin-C expression within the bursa mesenchyme. **(I)** The ectopic expression of tenascin-C was associated with abnormal lymphoid follicle formation, characterized by a reduction in chB6+ B cell precursors (Soós et al., 2025).

4.2.6. *In vitro* B cell migration is inhibited by tenascin-C

To assess the inhibitory role of tenascin-C in embryonic B cell migration, we performed *in vitro* migration assays using E13 bursal folds explanted onto the surface of cell culture dishes coated with either 20 ug/ml fibronectin or 10 ug/ml tenascin-C (Fig. 16A). Non-coated cell culture dishes served as controls. At this developmental stage, bursal folds are colonized by a large number of CXCR4+ B cell precursors (Fig. 16B). B cell emigration was stimulated by the addition of 100 ng/ml CXCL12 to the culture medium, a chemokine ligand known to induce robust chemotaxis in bursal B cells (Laparidou et al., 2020; Nagy et al., 2020). Stimulation with CXCL12 on non-coated tissue culture dishes resulted in limited emigration of CXCR4+ B cells (Fig. 16C). The presence of fibronectin strongly supports the migration of CXCR4+ B cells from the explant. Cells develop numerous membrane protrusions, indicating an active migratory state (Fig. 16D, inset). In contrast, the presence of tenascin-C markedly reduced the emigration of CXCR4+ B cells, associated with a round morphology (Fig. 16E, inset). The distance of the migratory front on different ECM surfaces was quantified from the border of the explants, with a significant difference between tenascin-C (220.6 ± 17.81 μm) and fibronectin (1098 ± 29.63 μm) coated conditions (Fig. 16F). Although the initial egress of CXCR4+ B cells from the explant occurred in all experimental conditions, sustained migration was specifically blocked in the presence of tenascin-C.

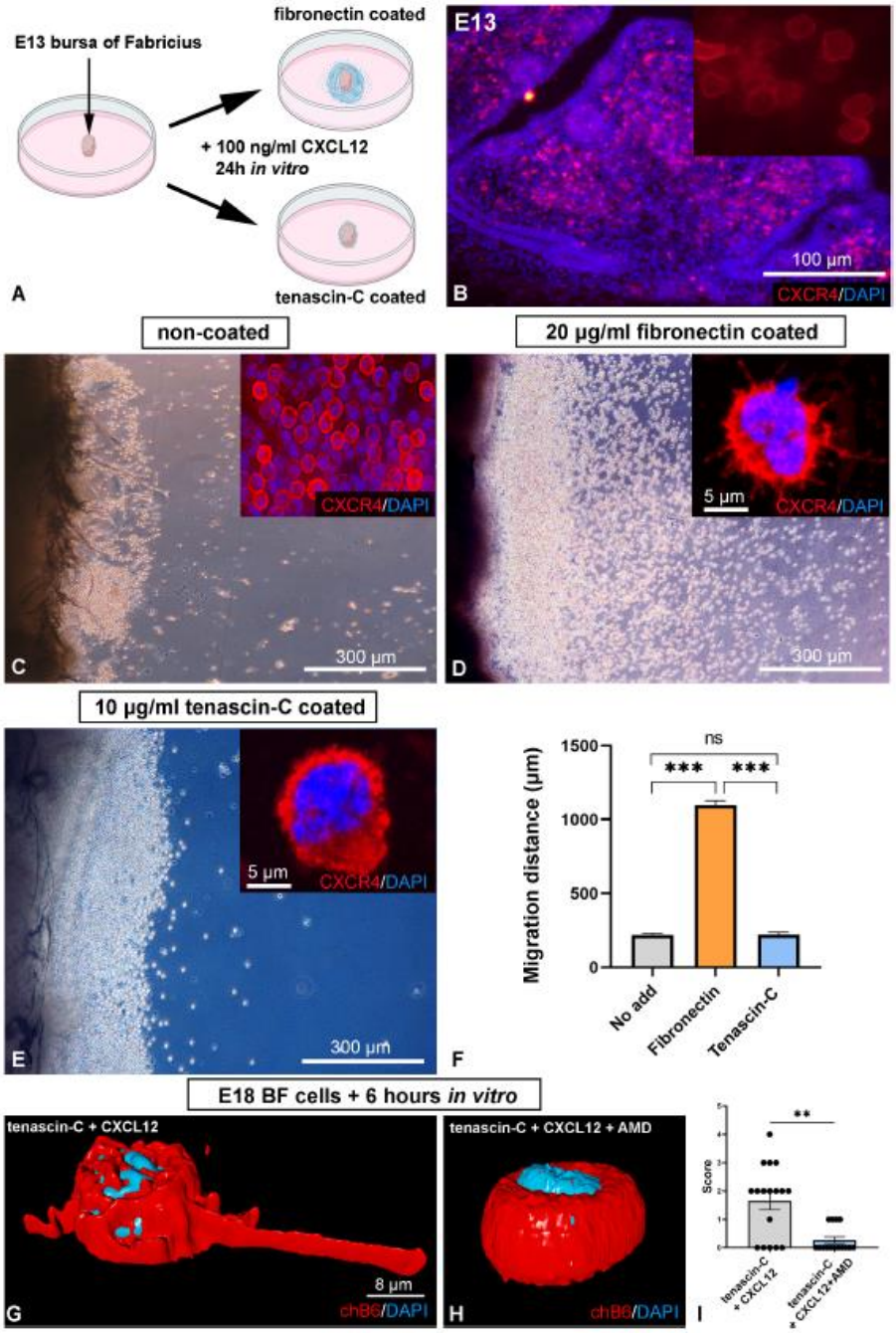


Figure 16. Effect of tenascin-C and tenascin-C-bound CXCL12 on B cell migration and adhesion. (A) Schematic illustration of embryonic BF organ culture experiments. **(B)** E13 chicken bursal folds containing CXCR4+ B cells were used to study cell migration induced by the CXCL12 chemokine. **(C)** CXCR4+ bursal cells show limited migration on untreated plastic cell culture dish surface in response to 100 ng/ml CXCL12. The inset shows a magnified view of CXCR4+ cells (red). DAPI (blue) was used for nucleus staining. **(D)** Coating the plastic surface with 20 µg/ml fibronectin induces robust CXCR4+

cell migration from the explant. Note the presence of extensive microvilli and filopodia on the surface of a CXCR4+ cell (inset). **(E)** In contrast, the presence of tenascin-C markedly inhibits CXCL12-induced cell migration, the CXCR4+ cells were spherical (inset). **(F)** Quantitative analysis of the migration distance of CXCR4+ cells for each experimental group. Data presented with the standard error of the mean. **(G)** CXCR4+/chB6+ B cells isolated from E18 BF and cultured on the surface of CXCL12 immobilized to tenascin-C-induced polarization of B cells with long filopodia, **(H)** which is effectively blocked by treatment with the CXCR4 receptor antagonist AMD3100, where B cells were spherical. **(I)** Quantitative analysis of cell morphology in bursal B cells for each experimental group. The length of filopodia in chB6+ cells was counted in 20 different high-power (200×) fields in untreated (RMPI-1640 culture medium) and AMD3100-treated cultures. chB6+ cells with filopodia longer than the cell diameter were scored. These are representative images of the morphologic phenotypes observed across 3 separate experiments, each including screening at least 200 cells. Significance levels: **p<0.01, ***p<0.001, ns, not significant. Error bars represent the standard error of the mean (Soós et al., 2025).

4.2.7. CXCL12-Tenascin-C interactions influence B cell morphology

While the embryonic bursa of Fabricius does not contain tenascin-C, post-hatch and adult lymphoid follicles express tenascin-C in the cortex (Fig. 13A, B). Similar to tenascin-C in fully mature follicles, CXCL12 chemokine expression is restricted to the cortex. Recent *in utero* human and *in vivo* mouse studies revealed that tenascin-C immobilizes migrating T cells, and tumor-infiltrating leukocytes are retained in the stroma. Given the fact that tenascin-C possesses conserved motifs for binding CXCL12 (Domaingo et al., 2023; Murdamoothoo et al., 2021) we also analyzed the effect of matrix-bound CXCL12 on bursal B cells. In control experiments, isolated bursal B cells seeded on tenascin-C-CXCL12 double-coated surface developed extensive filopodia and long, thin cytoplasmic protrusions (Fig. 16G, I). In contrast, blocking CXCR4 function with the receptor antagonist AMD3100, blocked CXCL12-induced cell polarization, characterized by the absence of filopodia formation, and B cells maintained a round, non-polarized morphology (Fig. 16H, I). These data indicate that tenascin-C is not only a structural scaffold in the follicular cortex but also functions as a regulatory ECM protein that modulates CXCR4-CXCL12 signaling in the cortical microenvironment.

5. DISCUSSION

Lymphoid organogenesis is a dynamic, highly controlled process during vertebrate embryogenesis, composed of a series of cellular interactions that result in the formation of primary lymphoid organs, which serve as developmental sites for the production of lymphoid cells from blood-borne progenitors and secondary lymphoid organs (SLOs), which act as primary sites for immune cell activation in adults. The immune system has two arms: the natural, innate immune system, which develops first, and the highly specialized adaptive immune system, which develops later during embryogenesis. Cells of the adaptive immune system in higher vertebrates are generated in specialized lympho-epithelial organs that serve as primary maturation sites for the generated lymphocyte pool. While the thymus universally serves as the T cell maturation site in all jawed vertebrates, B cells differentiate in anatomically diverse locations. Although the bone marrow is the central site for most mammals, species such as sheep, cattle, and rabbits primarily rely on specialized gut-associated lymphoid tissues to generate their early B cell repertoire (Abdou and Abdou, 1972; Abdou and Richter, 1970; Pospisil and Mage, 2011; Reynaud et al., 1991; Yasuda et al., 2006). An evolutionarily unique strategy is present in birds, where the generation of immunocompetent B cells occurs in the bursa of Fabricius. The specialized microenvironment that guides maturation of B cell precursors in the bursa is dependent on incoming blood-borne cells, which seed the bursal mesenchyme and induce the epithelium to form epithelial follicle buds.

Bursal hematopoietic colonization has been described as a two-step process: colonization of CSF1R+/MHCII+/74.3+ dendritic cell precursors to the epithelium drives the formation of epithelial follicle buds, which is followed by colonization of chB6+/CXCR4+ B cells and the transition to lympho-epithelial tissue, where further maturation and proliferation of early B cells takes place. Despite extensive characterization of early bursal hematopoietic colonization (Dóra et al., 2017; Houssaint et al., 1976; Le Douarin et al., 1975; Nagy et al., 2004a) several questions arise about the identity of the first immigrating blood-borne population. At the onset of bursal folliculogenesis, the presence of a previously uncharacterized EIV-E12+ cell population was observed, a population which was later

termed dendritic cell precursors (Oláh and Nagy, 2013; Pharr et al., 1995b). In post-hatch chicken, however, the antigen labels most bursal cells and is expressed in B cell-rich areas of secondary lymphoid organs (Felfoldi et al., 2015). Performing extensive immunostainings and immunoelectron microscopy with the available lympho-myeloid specific antibodies, we confirm that a distinct population of CD45+/EIV-E12+ cells is the first to appear in the bursal mesenchyme and colonize the surface epithelium on E10, resulting in the formation of epithelial buds. Further characterization in *CSF1R*-eGFP transgenic embryos reveals the presence of a population of EIV-E12+/*CSF1R*-eGFP- bursal cells that precede the entry of CD45+/*CSF1R*-eGFP+ ramified cells to the surface epithelium. Once EIV-E12+/*CSF1R*-eGFP- cells reach the bursal epithelium, sequential induction of follicle bud formation takes place, followed by the entry of *CSF1R*-eGFP-expressing ramified cells that together shape the follicular microenvironment prior to colonization of chB6+/IgM+ B cell precursors.

Although several studies have linked EIV-E12+ cells in the early bursal mesenchyme to dendritic cell precursors (Oláh and Nagy, 2013; Pharr et al., 1995b) a comprehensive study following the fate of early bursal EIV-E12+ cells in the follicular microenvironment was still lacking. Using duck-chicken CAM grafting experiments, we demonstrate that EIV-E12+ cells present in the early chicken BF colonize the surface epithelium and later become a transient cell population in the epithelial follicles, without the capacity to differentiate to dendritic cells or B cells. Based on this observation, we hypothesized that, similar to mammalian lymphoid tissue inducer cells (LTi) that orchestrate secondary lymphoid organ formation in mammalian embryos, EIV-E12+ cells in the avian bursa are the inducers for epithelial follicle bud formation. In a similar mechanism, blood-borne progenitors in the developing mammalian thymus were recently described to induce maturation of medullary thymic epithelial cells and ensure T cell-specific tissue homeostasis. These thymic cells are primed towards the LTi lineage, express *Rorc, Cd4, Cxcr5, Il7rα*, *Ltb,* and have a restricted differentiation potential, generating invariant T cells or thymic LTi (Elsaid et al., 2021; Ishizuka et al., 2016). Because EIV-E12+ cells colonize the bursal primordium prior to the arrival of B cell and dendritic cell precursors, we hypothesize that they function as avian analogs of mammalian lymphoid tissue inducer cells (LTi).

In mammalian models, LTi cells are characterized by the expression of interleukin-7 receptor-α (IL7R-α), neuropilin, and CXCR5, with species-specific variations in CD4 expression (Cupedo et al., 2002; Shikhagaie et al., 2017; van de Pavert, 2023). Immunofluorescence analysis of E12 chicken BF revealed that EIV-E12+ cells do not express these traditional mammalian LTi markers. While CD4 and IL7R-α were present on T cells and neuropilin-stained blood vessels in the BF, EIV-E12 immunoreactive cells were negative for these surface molecules.

Major signals that guide migration of LTi cells to sites of secondary lymphoid organ formation in mammals are RANK-RANKL (Cupedo and Mebius, 2005; Koning and Mebius, 2012), lymphotoxin-LTβR (Eberl et al., 2004), and CXCR5-CXCL13-mediated processes (Finke et al., 2002). Recent studies have uncovered the mechanism by which bursal B cells migrate to the epithelial follicle buds, which relies on the dynamic expression of the CXCL12 chemokine in bursal follicles (Laparidou et al., 2020; Nagy et al., 2020). Unlike B cells, EIV-E12+ cells do not express the CXCR4 receptor. Uncovering the developmental cues that guide migration of the earliest inducer cell population needs further elaboration. Possible candidates would be CXCL13 or CCL20 and their cognate receptors CXCR5 and CCR6, which have been demonstrated to facilitate inductive steps of secondary lymphoid organ formation in mammals (Finke et al., 2002; Kaiser et al., 2005; Velaga et al., 2009) and have also been confirmed to be present in chicken (Kaiser et al., 2005).

Chemical B cell depletion, complemented by CRISPR/Cas9 gene-edited RAG1 knockout systems has been extensively used to generate immunodeficient chicken model systems (Eskola, 1977; Lee et al., 2022). Similarly, systemic or local testosterone-propionate treatment results in the development of bursaless birds, via preventing the differentiation of bursal secretory dendritic cells and consequently the formation of dendro-epithelial tissue that is indispensable for further maturation of B cells within the bursa (Nagy and Oláh, 2009; Oláh et al., 1986). Despite the absence of these blood-borne populations in both systems, abortive bursal epithelial buds were reported with scattered dark cells in the follicles (Oláh et al., 1986; Soos et al., 1990). Here, we confirm that treating embryonic bursa primordia with AMD3100, the selective antagonist of the CXCR4 chemokine receptor, results in the formation of B cell-depleted bursa follicles but does not affect immigration of EIV-E12+

cells and 74.3+ dendritic cells in the forming follicles. Similarly, testosterone-propionate-mediated depletion of 74.3+ dendritic cells in the embryonic bursa does not influence clustering of EIV-E12+ cells and has no inhibitory effect on early stages of follicle bud development. This is also supported by a recent study in *CSF1R*-KO chicken, in which the formation of rudimentary epithelial follicles is not affected by the genetic ablation of CSF1R+ dendritic cell precursors (Wu et al., 2026). Together, these findings suggest that clustering of EIV-E12+ cells in the bursal epithelium represents the earliest step of folliculogenesis in the chicken bursa of Fabricius, without the need for other lympho-myeloid cell types. Quail-chick epithelial-mesenchymal recombination experiments further demonstrate the inducer role of EIV-E12+ cells with the capacity to colonize the bursal surface epithelium and induce the formation of lymphoid follicles.

Taken together, these data redefine the hierarchy of bursal follicle development. While B cells and dendritic cell precursors are essential for the establishment of the follicular microenvironment, they are not the primary drivers of follicle bud initiation. Instead, EIV-E12+ cells function as a distinct population that drives early epithelial colonization and follicle bud formation independently of other myeloid and lymphoid lineages. Based on these observations, we propose a novel, three-step colonization model for early BF development. During **Stage I**, mesenchymal cells aggregate beneath the bursal surface epithelium, which are stimulated by a yet undefined signal to express CXCL12, alkaline phosphatase, and various proteases. These molecular changes modify the subepithelial mesenchyme to become receptive to blood-borne CD45+/EIV-E12+ cells. Colonization of the surface epithelium initiates follicle bud formation, which demonstrates the follicle inducer role of the first incoming cells. In **Stage II**, CD45+/CSF1R+/74.3+ myeloid cells colonize these emerging buds to establish a temporary dendro-epithelial tissue. These CD45+/CSF1R+/74.3+ cells later differentiate into mature bursal secretory dendritic cells in the follicular medulla and accumulate in the expanding follicle buds alongside CD45+/TIM4+ macrophages. In **Stage III**, chB6+/IgM+/BAFF-R+ B cell precursors infiltrate the developing follicles (Fig. 17).

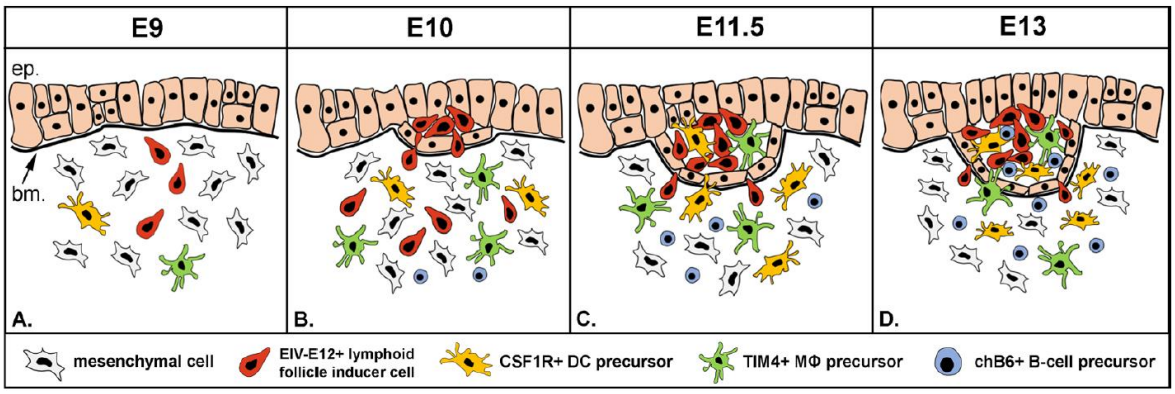


Figure 17. New model of folliculogenesis in the bursa of Fabricius. (A, B) Phase I: Blood-borne CD45+/EIV-E12+ lymphoid follicle inducer cells are the first to reach the surface epithelium on E10, cross the basement membrane, and induce lymphoid follicle bud formation. **(C) Phase II**: CSF1R+ dendritic cells and TIM4+ macrophage precursors colonize the developing follicle buds on E11.5. **(D) Phase III**: chB6+/IgM+ B cell precursors first enter the follicle buds on E13. ep, epithelium; bm, basement membrane; DC, dendritic cell; MF, macrophage (Szőcs et al., 2024).

This sequential colonization of the developing BF recapitulates the basic steps of secondary lymphoid organogenesis in mammals. **Step I**: LTi cells migrate to designated sites in the embryo and, through a series of highly controlled molecular crosstalk, form the initial lymphoid organ anlagen acting as critical initiators for secondary lymphoid tissue formation (van de Pavert, 2021). **Step II**: Through their specific chemokine production, resident stromal cells produce homeostatic chemokines, triggering the differentiation of high endothelial venules, stromal cell networks, and resident dendritic cell populations, which provide the essential microenvironmental support to attract lymphocytes (Calabrò et al., 2026). **Step III**: Naive lymphocytes are directed to the lymphoid organ anlagen by the established chemokine gradients to form spatially distinct T cell-zones and B cell follicles, with the capacity to differentiate to effector cells upon activation by antigen exposure (Ager, 2017; Buettner and Lochner, 2016; Schulz et al., 2016).

Embryonic LTi cells and postnatal LTi-like cells that drive the development of secondary lymphoid organs and orchestrate tertiary lymphoid structure formation in mammals and humans are a highly heterogeneous population, with phenotypic markers that

vary among species (Vivier et al., 2018). Single-cell transcriptomic analyses reveal several cell surface markers (Ishizuka et al., 2016), among which CXCR5, the chemokine receptor for CXCL13, is uniformly expressed by these cells and has a predominant role in guiding LTi cells to developing lymphoid structures (Finke et al., 2002; Velaga et al., 2009) and facilitates lymphoid tissue maintenance (Sécca et al., 2021). Taking advantage of transcriptomic platforms, complemented by cell-sorting and adoptive cell transfer studies, we plan to elucidate the origins of avian LTi cells and the developmental cues that guide lymphoid organogenesis, a process that appears to be evolutionarily conserved across avian and mammalian species. Our findings provide a detailed immunophenotypic characterization of early bursal LTi cells, complemented by embryo manipulation experiments, which are the first to demonstrate the inductive role of this population in avian follicle bud formation in the bursa of Fabricius.

Upon colonization of the follicles by chB6+/IgM+ B cell precursors, a phase of rapid cell expansion begins, which results in the emergence of a B cell pool that undergoes repeated somatic gene conversion events within bursal follicles (Ratcliffe, 2006; Ratcliffe and Härtle, 2022). In post-hatch animals, bursal lymphoid follicles undergo a second morphogenetic event, marked by the migration of B cells from the epithelial compartment to form the cortex of bursal lymphoid follicles (Oláh et al., 2022; Paramithiotis and Michael, 1994). In post-hatch animals, peripheral lymphoid tissues are continuously seeded by cortical B cells, moving first into the circulation and subsequently populating B cell regions within the spleen, thymus, and cecal tonsils (Paramithiotis and Michael, 1994; Paramithiotis and Ratcliffe, 1994). This continuous migration is the key to sustaining a steady pool of mature B cells required for effective adaptive immune responses. Despite its indispensable role in the immunocompetence of birds, the ontogeny and cellular composition of the cortical compartment have remained relatively underexplored.

Previous studies have demonstrated that the cortex of bursal follicles is a microenvironment enriched with the CXCL12 chemokine, which induces the migration of CXCR4+ medullary B cells into cortical zones (Laparidou et al., 2020; Nagy et al., 2020). We demonstrate that mesenchymal reticular cells in the cortex not only form a structural scaffold, but they are also the source of the CXCL12 chemokine in mature bursal follicles.

This high local CXCL12 concentration selectively recruits CXCR4-immunoreactive B cells from the follicular medulla. Double-immunofluorescence imaging revealed a unique spatial organization: CXCL12-producing stromal cells align closely with CXCR4^{high} B cells in the peripheral cortex, whereas CXCR4$^{low/dim}$ B cells reside adjacent to the cortico-medullary junction, where the expression of tenascin-C, a glycoprotein-type extracellular matrix protein, is the highest. We demonstrate that tenascin-C is uniquely expressed in the inner region of the cortical compartment of adult BF follicles, and appears before hatching, coinciding with the formation of the cortex. Unlike other ECM proteins, which are uniformly distributed during bursal development, tenascin-C exhibits a highly specific and dynamic expression pattern, suggesting a specialized regulatory role in establishing the cortical microenvironment.

Using *in vitro* organ culture and cell migration assays, we confirm that tenascin-C functions as an inhibitory matrix component for B cell migration. Furthermore, *in vivo* experiments using retrovirus-mediated ectopic expression of *Shh* demonstrate that tenascin-C expression impairs follicular development, highlighting its role in regulating B cell precursor homing and localization. These results suggest that the absence of tenascin-C during embryonic stages facilitates the migration and homing of CXCR4^{high} B-cell precursors to the BF primordium. As development progresses, the emergence of tenascin-C within the cortical region likely creates a barrier that modifies the migratory behavior of cortical B cells. This is consistent with studies in other systems, where tenascin-C has been shown to interact with CXCL12 to modulate lymphocyte migration by forming molecular barriers (da Silva et al., 2021; Murdamoothoo et al., 2021).

The presence of tenascin-C in the cortex could similarly act as a regulatory checkpoint, preventing excessive B cell emigration and maintaining proper follicular compartmentalization. Our observations also highlight the complementary expression patterns of tenascin-C, CXCL12, and CXCR4 in the BF. Cortical mesenchymal reticular cells produce CXCL12, which has been shown to play a critical role in attracting CXCR4-expressing B cells (Nagy et al., 2020; Laparidou et al., 2020). However, the inhibitory effect of tenascin-C on CXCL12 function underscores the complexity of ECM-chemokine interactions in shaping B cell dynamics. The observed downregulation of CXCR4 in cortical

B cells adjacent to the cortico-medullary border and near capillaries suggests a mechanism by which B cells exit the CXCL12-rich microenvironment of the cortex to emigrate to peripheral lymphoid organs. This is in agreement with previous findings that peripheral B cells originate from the cortical compartment of the BF follicles (Lassila, 1989; Paramithiotis and Ratcliffe, 1994).

Whether a chemokine or growth factor is soluble or bound to the extracellular matrix regulates how it influences cell migration and adhesion. Here, we report that tenascin-C immobilized CXCL12 triggers a morphological shift, causing CXCR4+ B cells to polarize and extend long filopodia. Inhibiting CXCR4 function by the selective antagonist AMD3100 counteracts this phenotype, demonstrating that the functional CXCR4-CXCL12 signaling is essential for tenascin-C-mediated B cell adhesion. This specialized microenvironment around cortical blood vessels in the avian bursal cortex directly models the endosteal and sinusoidal niches found in the mammalian bone marrow, where CXCL12-abundant reticular (CAR) cells establish the high local CXCL12 concentration, while also secreting tenascin-C (Nakamura-Ishizu et al., 2012). We hypothesize that this evolutionarily conserved mechanism retains immature B cells within the specialized bursal stromal niche. This tightly regulated retention mechanism ensures that cells receive vital differentiation and survival signals before eventually responding to blood chemokines and exiting primary lymphoid organs. Our embryo surgery experiments and *in vitro* cultures provide a model in which tenascin-C and CXCL12 interact within the follicular cortex to establish distinct zones that regulate B-cell localization and migration. Our data suggest that the absence of tenascin-C in embryonic stages is crucial for $CXCR4^{high}$ B cell precursor homing, while its later expression creates a migration-restrictive environment necessary for follicular compartmentalization.

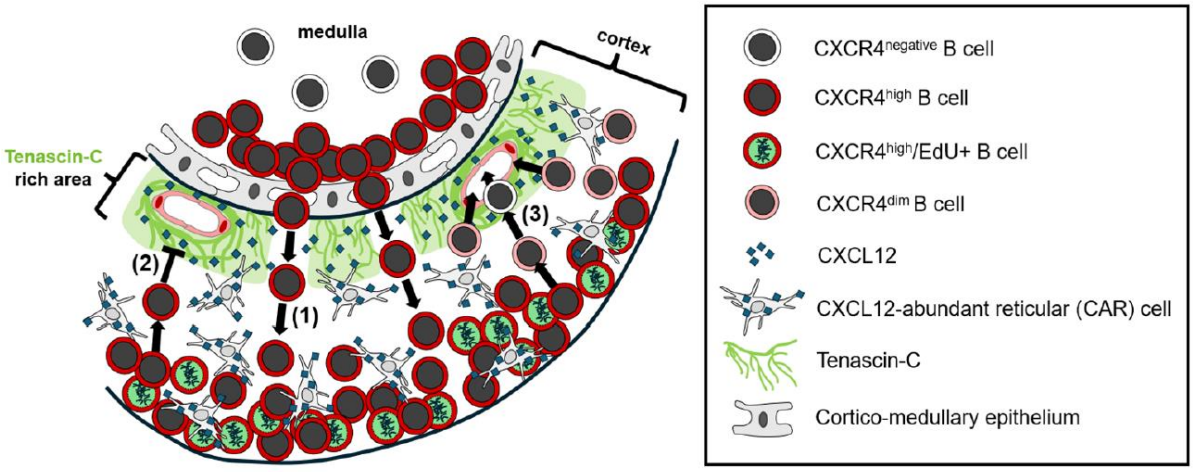


Figure 18. Schematic illustration of B cell migration in the cortex of bursal follicles. **(1)** CXCR4^{high} medullary B cells migrate towards high concentrations of CXCL12 in the cortex, along tenascin-C free zones between cortical capillaries. CXCL12-abundant reticular (CAR) cells within the cortex establish the high local chemokine concentrations. Soluble CXCL12 interacts with extracellular tenascin-C, forming CXCL12-rich zones around cortical capillaries. **(2)** Expansion of CXCR4^{high} B cells occurs in outer cortical regions, and CXCL12-rich zones around cortical capillaries prevent premature B cell emigration towards extra-bursal sites. **(3)** Bursal B cell emigration is dependent on the downregulation of the CXCR4 receptor, allowing cell migration through CXCL12-rich inner cortical zones. CXCR4$^{low/dim}$ B cells reach the periphery through cortical capillaries (Soós et al., 2025).

Taken together, the morphological and structural compartmentalization of the bursa of Fabricius relies on sequential, tightly regulated interactions between mesenchymal stroma and infiltrating hematopoietic lineages. While the initial steps of follicle development require the recruitment of EIV-E12+ lymphoid follicle inducer cells to the bursa primordium, the subsequent maturation and egress of B cells to peripheral sites are dynamically controlled by a conserved ECM-chemokine framework that regulates lymphocyte development.

6. CONCLUSION

Using avian embryo manipulation and *in vitro* studies, we characterized the ontogeny, cellular architecture, and microenvironmental regulation of lymphoid follicle development in the avian bursa of Fabricius, showing how specific lympho-myeloid populations sequentially colonize the embryonic bursa to initiate lymphoid follicle formation. We also elucidate the spatial organization of the cortical compartment, highlighting how resident stromal cells, extracellular matrix proteins, and chemokines govern B cell migration and compartmentalization.

Our results show that:

- Bursal lymphoid follicle formation is initiated by a novel CD45+/EIV-E12+ blood-borne cell population, which acts as the lymphoid follicle inducer cell during bursal ontogenesis.
- Using embryo manipulation and chick-quail tissue recombination, we demonstrate that EIV-E12+ cells represent a transient, inductive population in the bursa that does not differentiate into dendritic cells, macrophages, or B cells.
- The cortex of bursal lymphoid follicles is supported by a distinct population of desmin+/vimentin+ reticular cells that are the major source of the CXCL12 chemokine in the adult bursa.
- Unlike other ECM proteins, tenascin-C expression first appears in late embryonic stages and is restricted to the inner mesenchymal region in the cortex of adult lymphoid follicles. This distribution creates a complementary expression pattern with CXCR4 immunoreactive cortical B cells.
- Tenascin-C regulates CXCL12-induced embryonic B cell migration *in vitro.*
- *In ovo* Shh-RCAS-retrovirus-induced ectopic tenascin-C overexpression in the embryonic bursa severely disrupts B cell colonization and inhibits lymphoid follicle formation.
- Tenascin-C - CXCL12 interactions control B cell egress from the cortex of bursal lymphoid follicles.

7. SUMMARY

The bursa of Fabricius (BF) is a unique primary lymphoid organ essential for B cell development in birds, that provides a highly specialized and selective microenvironment for the proliferation and differentiation of early precursors. While the function of the medulla in bursal lymphoid follicles is well characterized, the steps of BF organogenesis from the initial induction of epithelial follicle buds to the emergence and regulatory function of the cortical compartment are still not fully understood. Here, we characterize two critical, temporally distinct phases of BF development: the inductive mechanisms that drive lymphoid follicle bud formation and post-hatch extracellular matrix-chemokine interactions that govern B cell migration and egress to the periphery.

Using wild-type and *CSF1R*-eGFP transgenic chick embryos, combined with chick-duck chimeras and chick-quail tissue recombination, we identify a novel EIV-E12+ lymphoid follicle inducer cell population. Experimental depletion models demonstrate that these cells are distinct from B cell and dendritic cell precursors and are capable of inducing follicle bud formation.

Following early follicle formation, the BF undergoes further structural maturation with the development of the follicular cortex. Using immunochemistry, RNAscope *in situ* hybridization, we show that the cortex of lymphoid follicles is supported by desmin+/vimentin+ mesenchymal reticular cells that secrete CXCL12 and tenascin-C in the cortical microenvironment. Embryo manipulation experiments using a Shh-RCAS retrovirus reveal that tenascin-C acts as a potent regulator of B cell migration and experimental overexpression actively disrupts B cell homing and follicle formation. In the adult BF, tenascin-C interacts with the CXCL12 chemokine to regulate B cell egress. We show that CXCR4^{high} B cells must downregulate the CXCR4 receptor to successfully navigate through the CXCL12 and tenascin-C-rich cortical network, before they can exit the bursa to reach the periphery.

Together, these data present a comprehensive model of BF ontogenesis and provide vital new insights into the dynamic, stage-specific microenvironmental cues that control primary lymphoid organ development.

8. REFERENCES

Abdou, N. I. and Abdou, N. L. (1972). Bone marrow: The bursa equivalent in man? *Science (1979).* **175**, 446–448.

Abdou, N. I. and Richter, M. (1970). The role of bone marrow in the immune response. *Adv. Immunol.* **12**, 201–70.

Ager, A. (2017). High Endothelial Venules and Other Blood Vessels: Critical Regulators of Lymphoid Organ Development and Function. *Front. Immunol.* **8**,.

Akbareian, S. E., Nagy, N., Steiger, C. E., Mably, J. D., Miller, S. A., Hotta, R., Molnar, D. and Goldstein, A. M. (2013). Enteric neural crest-derived cells promote their migration by modifying their microenvironment through tenascin-C production. *Dev. Biol.* **382**, 446–456.

Arakawa, H. and Buerstedde, J. M. (2004). Immunoglobulin Gene Conversion: Insights from Bursal B Cells and the DT40 Cell Line. *Developmental Dynamics* **229**, 458–464.

Balic, A., Garcia-Morales, C., Vervelde, L., Gilhooley, H., Sherman, A., Garceau, V., Gutowska, M. W., Burt, D. W., Kaiser, P., Hume, D. A., et al. (2014). Visualisation of chicken macrophages using transgenic reporter genes: Insights into the development of the avian macrophage lineage. *Development (Cambridge)* **141**, 3255–3265.

Balic, A., Chintoan-Uta, C., Vohra, P., Sutton, K. M., Cassady-Cain, R. L., Hu, T., Donaldson, D. S., Stevens, M. P., Mabbott, N. A., Hume, D. A., et al. (2019). Antigen sampling csf1r-expressing epithelial cells are the functional equivalents of mammalian m cells in the avian follicle-associated epithelium. *Front. Immunol.* **10**, 1–16.

Benatar, T., Lacampo, S., Tkalec, L. and Ratcliffe, M. J. H. (1991). Expression of immunoglobulin genes in the avian embryo bone marrow revealed by retroviral transformation. *Eur. J. Immunol.* **21**, 2529–2536.

Boehm, T. (2025). Understanding vertebrate immunity through comparative immunology. *Nat. Rev. Immunol.* **25**, 141–152.

Buettner, M. and Lochner, M. (2016). Development and function of secondary and tertiary lymphoid organs in the small intestine and the colon. *Front. Immunol.* **7**, 1–11.

Calabrò, A., De Pasquale, C., Drommi, F., Giusto, E., Tamburini, S., Vento, G., Yamazaki, S., Campana, S. and Ferlazzo, G. (2026). Dendritic Cells: key controllers of lymphoid tissue organization. *Immunol. Lett.* **278**, 107111.

Cherrier, M., Sawa, S. and Eberl, G. (2012). Notch, Id2, and RORγt sequentially orchestrate the fetal development of lymphoid tissue inducer cells. *Journal of Experimental Medicine* **209**, 729–740.

Christensen, J. L., Wright, D. E., Wagers, A. J. and Weissman, I. L. (2004). Circulation and Chemotaxis of Fetal Hematopoietic Stem Cells. *PLoS Biol.* **2**, e75.

Ciriaco, E., Píñera, P. P., Díaz-Esnal, B. and Laurà, R. (2003). Age-Related Changes in the Avian Primary Lymphoid Organs (Thymus and Bursa of Fabricius). *Microsc. Res. Tech.* **62**, 482–487.

Constantinides, M. G., McDonald, B. D., Verhoef, P. A. and Bendelac, A. (2014). A committed precursor to innate lymphoid cells. *Nature* **508**, 397–401.

Cooper, M. D., Peterson, R. D. A. and Good, R. A. (1965). Delineation of the Thymic and Bursal Lymphoid Systems in the Chicken. *Nature* **205**, 143–146.

Cupedo, T. and Mebius, R. E. (2005). Cellular Interactions in Lymph Node Development. *The Journal of Immunology* **174**, 21–25.

Cupedo, T., Kraal, G. and Mebius, R. E. (2002). The role of CD45+CD4+CD3- cells in lymphoid organ development. *Immunol. Rev.* **189**, 41–50.

da Silva, P. H. R., Borges, B. C., Uehara, I. A., Soldi, L. R., de Araújo, R. A. and Silva, M. J. B. (2021). Chemokines and the extracellular matrix: Set of targets for tumor development and treatment. *Cytokine* **144**,.

Das, A., Ding, Y., Harly, C. and Bhandoola, A. (2026). The development of innate lymphoid cells. *Nat. Immunol.* **27**, 401–412.

Dieterlen Lievre, F. (1975). On the origin of haemopoietic stem cells in the avian embryo: an experimental approach. *J. Embryol. Exp. Morphol.* **33**, 607–619.

Domaingo, A., Jokesch, P., Schweiger, A., Gschwandtner, M., Gerlza, T., Koch, M., Midwood, K. S. and Kungl, A. J. (2023). Chemokine Binding to Tenascin-C Influences Chemokine-Induced Immune Cell Migration. *Int. J. Mol. Sci.* **24**,.

Dóra, D., Fejszák, N., Goldstein, A. M., Minkó, K. and Nagy, N. (2017). Ontogeny of ramified CD45 cells in chicken embryo and their contribution to bursal secretory dendritic cells. *Cell Tissue Res.* **368**, 353–370.

Dunon, D., Allioli, N., Vainio, O., Ody, C. and Imhof, B. A. (1998). Renewal of thymocyte progenitors and emigration of thymocytes during avian development. *Dev. Comp. Immunol.* **22**, 279–287.

Eberl, G., Marmon, S., Sunshine, M. J., Rennert, P. D., Choi, Y. and Littmann, D. R. (2004). An essential function for the nuclear receptor RORγt in the generation of fetal lymphoid tissue inducer cells. *Nat. Immunol.* **5**, 64–73.

Eberl, G., Colonna, M., Di Santo, J. P. and McKenzie, A. N. J. (2015). Innate lymphoid cells. Innate lymphoid cells: a new paradigm in immunology. *Science* **348**, aaa6566.

Elsaid, R., Meunier, S., Burlen-Defranoux, O., Soares-da-Silva, F., Perchet, T., Iturri, L., Freyer, L., Vieira, P., Pereira, P., Golub, R., et al. (2021). A wave of bipotent T/ILC-restricted progenitors shapes the embryonic thymus microenvironment in a time-dependent manner. *Blood* **137**, 1024–1036.

Erhard, M. H., Von Quistorp, I., Schranner, I., Jüngling, A., Kaspers, B., Schmidt, P. and Kühlmann, R. (1992). Development of specific enzyme-linked immunosorbent

antibody assay systems for the detection of chicken immunoglobulins G, M, and A using monoclonal antibodies. *Poult. Sci.* **71**, 302–310.

Eskola, J. (1977). Cell transplantation into immunodeficient chicken embryos. Reconstituting capacity of cells from the yolk sac at different stages of development and from the liver, thymus, bursa of Fabricius, spleen and bone marrow of 15-day embryos. *Immunology* **32**, 467–74.

Fagraeus, A. (1947). Plasma Cellular Reaction and its Relation to the Formation of Antibodies in vitro. *Nature* **159**, 499–499.

Fejszák, N., Kocsis, K., Halasy, V., Szőcs, E., Soós, Á., Roche, D. von La, Härtle, S. and Nagy, N. (2022). Characterization and functional properties of a novel monoclonal antibody which identifies a B cell subpopulation in bursa of Fabricius. *Poult. Sci.* **101**, 1–12.

Felfoldi, B., Pharr, G. T., Bodi, I., Olah, I., Alugubelly, N., Nuthalapat, N. and Fejszak, N. (2015). Monoclonal Antibody EIV-E12 Recognizes a Glycoprotein Antigen, Which Differs from the B-Cell-Specific chB6 (Bu-1) Antigen. *Int. J. Poult. Sci.* **14**, 479–484.

Finke, D., Acha-Orbea, H., Mattis, A., Lipp, M. and Kraehenbuhl, J. P. (2002). CD4+CD3− Cells Induce Peyer's Patch Development. *Immunity* **17**, 363–373.

Fütterer, A., Mink, K., Luz, A., Kosco-Vilbois, M. H. and Pfeffer, K. (1998). The lymphotoxin β receptor controls organogenesis and affinity maturation in peripheral lymphoid tissues. *Immunity* **9**, 59–70.

Ganuza, M., Hall, T., Finkelstein, D., Chabot, A., Kang, G. and McKinney-Freeman, S. (2017). Lifelong haematopoiesis is established by hundreds of precursors throughout mammalian ontogeny. *Nat. Cell Biol.* **19**, 1153–1163.

Garcia-Morales, C., Rothwell, L., Moffat, L., Garceau, V., Balic, A., Sang, H. M., Kaiser, P. and Hume, D. A. (2014). Production and characterisation of a monoclonal antibody that recognises the chicken CSF1 receptor and confirms that expression is restricted to macrophage-lineage cells. *Dev. Comp. Immunol.* **42**, 278–285.

Gasteiger, G., Fan, X., Dikiy, S., Lee, S. Y. and Rudensky, A. Y. (2015). Tissue residency of innate lymphoid cells in lymphoid and nonlymphoid organs. *Science (1979).* **350**, 981–985.

Glick, B., Chang, T. and Jaap, R. (1956). The bursa of Fabricius and antibody production. *Poult. Sci.* **35**, 224–225.

Houssaint, E. (1987). Cell lineage segregation during bursa of Fabricius ontogeny. *The Journal of Immunology* **138**, 3626–3634.

Houssaint, E., Belo, M. and Le Douarin, N. M. (1976). Investigations on cell lineage and tissue interactions in the developing bursa of Fabricius through interspecific chimeras. *Dev. Biol.* **53**, 250–264.

Igyártó, B. Z., Nagy, N., Magyar, A. and Oláh, I. (2008). Identification of the avian B-cell-specific Bu-1 alloantigen by a novel monoclonal antibody. *Poult. Sci.* **87**, 351–355.

Ishizuka, I. E., Chea, S., Gudjonson, H., Constantinides, M. G., Dinner, A. R., Bendelac, A. and Golub, R. (2016). Single-cell analysis defines the divergence between the innate lymphoid cell lineage and lymphoid tissue-inducer cell lineage. *Nat. Immunol.* **17**, 269–276.

Jaffredo, T., Gautier, R., Brajeul, V. and Dieterlen-Lièvre, F. (2000). Tracing the progeny of the aortic hemangioblast in the avian embryo. *Dev. Biol.* **224**, 204–214.

Kaiser, P., Poh, T. Y., Rothwell, L., Avery, S., Balu, S., Pathania, U. S., Hughes, S., Goodchild, M., Morrell, S., Watson, M., et al. (2005). A genomic analysis of chicken cytokines and chemokines. *Journal of Interferon and Cytokine Research* **25**, 467–484.

Kasal, D. N. and Bendelac, A. (2021). Multi-transcription factor reporter mice delineate early precursors to the ILC and LTi lineages. *Journal of Experimental Medicine* **218**,.

Klose, C. S. N., Flach, M., Möhle, L., Rogell, L., Hoyler, T., Ebert, K., Fabiunke, C., Pfeifer, D., Sexl, V., Fonseca-Pereira, D., et al. (2014). Differentiation of Type 1 ILCs from a Common Progenitor to All Helper-like Innate Lymphoid Cell Lineages. *Cell* **157**, 340–356.

Koni, P. A., Sacca, R., Lawton, P., Browning, J. L., Ruddle, N. H. and Flavell, R. A. (1997). Distinct Roles in Lymphoid Organogenesis for Lymphotoxins α and β Revealed in Lymphotoxin β–Deficient Mice. *Immunity* **6**, 491–500.

Koning, J. J. and Mebius, R. E. (2012). Interdependence of stromal and immune cells for lymph node function. *Trends Immunol.* **33**, 264–270.

Kothlow, S., Mannes, N. K., Schaerer, B., Rebeski, D. E., Kaspers, B. and Schultz, U. (2005). Characterization of duck leucocytes by monoclonal antibodies. *Dev. Comp. Immunol.* **29**, 733–748.

Kothlow, S., Morgenroth, I., Graef, Y., Schneider, K., Riehl, I., Staeheli, P., Schneider, P. and Kaspers, B. (2006). Unique and conserved functions of B cell-activating factor of the TNF family (BAFF) in the chicken. *Int. Immunol.* **19**, 203–215.

Kothlow, S., Morgenroth, I., Tregaskes, C. A., Kaspers, B. and Young, J. R. (2008). CD40 ligand supports the long-term maintenance and differentiation of chicken B cells in culture. *Dev. Comp. Immunol.* **32**, 1015–1026.

Kowalski, W. J., Malkinson, M., Leslie, G. A. and Small, P. A. (1978). *The secretory immunological system of the fowl VI. THE EFFECT OF CHEMICAL BURSECTOMY ON IMMUNOGLOBULIN CONCENTRATION IN TEARS*.

Laparidou, M., Schlickenrieder, A., Thoma, T., Lengyel, K. and Schusser, B. (2020). Blocking of the CXCR4-CXCL12 Interaction Inhibits the Migration of Chicken B Cells Into the Bursa of Fabricius. *Front. Immunol.* **10**, 1–10.

Lassila, O. (1989). Emigration of B cells from chicken bursa of Fabricius. *Eur. J. Immunol.* **19**, 955–958.

Le Douarin, N. M., Houssaint, E., Jotereau, F. V. and Belo, M. (1975). Origin of hemopoietic stem cells in embryonic bursa of Fabricius and bone marrow studied through interspecific chimeras. *Proceedings of the National Academy of Sciences* **72**, 2701–2705.

Lee, S. H., Lillehoj, H. S., Jang, S. I., Baldwin, C., Tompkins, D., Wagner, B., Parcells, M., Del Cacho, E., Hong, Y. H., Min, W., et al. (2011). Development and characterization of mouse monoclonal antibodies reactive with chicken interleukin-2 receptor αlpha chain (CD25). *Vet. Immunol. Immunopathol.* **144**, 396–404.

Lee, K. Y., Choi, H. J., Park, K. J., Woo, S. J., Kim, Y. M. and Han, J. Y. (2022). Development and characterization of a CRISPR/Cas9-mediated RAG1 knockout chicken model lacking mature B and T cells. *Front. Immunol.* **13**, 1–18.

Lupetti, M., Dolfi, A., Giannessi, F., Bianchi, F. and Michelucci, S. (1990). Reappraisal of histogenesis in the bursal lymphoid follicle of the chicken. *American Journal of Anatomy* **187**, 287–302.

Madej, J. P., Chrzaogonekstek, K., Piasecki, T. and Wieliczko, A. (2013). New insight into the structure, development, functions and popular disorders of Bursa Fabricii. *Journal of Veterinary Medicine Series C: Anatomia Histologia Embryologia* **42**, 321–331.

Mansikka, A., Sandberg, M., Lassila, O. and Toivanen, P. (1990). Rearrangement of immunoglobulin light chain genes in the chicken occurs prior to colonization of the embryonic bursa of Fabricius. *Proc. Natl. Acad. Sci. U. S. A.* **87**, 9416–9420.

Masteller, E. L. and Thompson, C. B. (1994). B cell development in the chicken. *Poult. Sci.* **73**, 998–1011.

Masteller, E. L., Larsen, R. D., Carlson, L. M., Pickel, J. M., Nickoloff, B., Lowe, J., Thompson, C. B. and Lee, K. P. (1995). Chicken B cells undergo discrete developmental changes in surface carbohydrate structure that appear to play a role in directing lymphocyte migration during embryogenesis. *Development* **121**, 1657–1667.

McCormack, W. T., Tjoelker, L. W., Barth, C. F., Carlson, L. M., Petryniak, B., Humphries, E. H. and Thompson, C. B. (1989). Selection for B cells with productive IgL gene rearrangements occurs in the bursa of Fabricius during chicken embryonic development. *Genes Dev.* **3**, 838–847.

McCormack, W. T., Tjoelker, L. W. and Thompson, C. B. (1991). Avian B-cell development: Generation of an immunoglobulin repertoire by gene conversion. *Annu. Rev. Immunol.* **9**, 219–241.

McNagny, K. M., Pettersson, I., Rossi, F., Flamme, I., Shevchenko, A., Mann, M. and Graf, T. (1997). Thrombomucin, a novel cell surface protein that defines thrombocytes and multipotent hematopoietic progenitors. *J. Cell Biol.* **138**, 1395–407.

Mebius, R. E. (2003). Organogenesis of lymphoid tissues. *Nat. Rev. Immunol.* **3**, 292–303.

Meier, D., Bornmann, C., Chappaz, S., Schmutz, S., Otten, L. A., Ceredig, R., Acha-Orbea, H. and Finke, D. (2007). Ectopic Lymphoid-Organ Development Occurs through Interleukin 7-Mediated Enhanced Survival of Lymphoid-Tissue-Inducer Cells. *Immunity* **26**, 643–654.

Miller, J. (1961). IMMUNOLOGICAL FUNCTION OF THE THYMUS. *The Lancet* **278**, 748–749.

Murdamoothoo, D., Sun, Z., Yilmaz, A., Riegel, G., Abou-Faycal, C., Deligne, C., Velazquez-Quesada, I., Erne, W., Nascimento, M., Mörgelin, M., et al. (2021). Tenascin-C immobilizes infiltrating T lymphocytes through CXCL12 promoting breast cancer progression. *EMBO Mol. Med.* **13**, 1–21.

Nagy, N. and Oláh, I. (2009). Locally applied testosterone is a novel method to influence the development of the avian bursa of Fabricius. *J. Immunol. Methods* **343**, 97–102.

Nagy, N. and Oláh, I. (2010). Experimental evidence for the ectodermal origin of the epithelial anlage of the chicken bursa of Fabricius. *Development* **137**, 3019–3023.

Nagy, N., Magyar, A., Dávid, C., Gumati, M. K. and Oláh, I. (2001). Development of the follicle-associated epithelium and the secretory dendritic cell in the bursa of Fabricius of the guinea fowl (Numida Meleagris) studied by novel monoclonal antibodies. *Anatomical Record* **262**, 279–292.

Nagy, N., Magyar, A., Tóth, M. and Oláh, I. (2004a). Quail as the chimeric counterpart of the chicken: Morphology and ontogeny of the bursa of Fabricius. *J. Morphol.* **259**, 328–339.

Nagy, N., Magyar, A., Tóth, M. and Oláh, I. (2004b). Origin of the bursal secretory dendritic cell. *Anat. Embryol. (Berl).* **208**, 97–107.

Nagy, N., Bódi, I. and Oláh, I. (2016a). Avian dendritic cells: Phenotype and ontogeny in lymphoid organs. *Dev. Comp. Immunol.* **58**, 47–59.

Nagy, N., Barad, C., Graham, H. K., Hotta, R., Cheng, L. S., Fejszak, N. and Goldstein, A. M. (2016b). Sonic hedgehog controls enteric nervous system development by patterning the extracellular matrix. *Development (Cambridge)* **143**, 264–275.

Nagy, N., Busalt, F., Halasy, V., Kohn, M., Schmieder, S., Fejszak, N., Kaspers, B. and Härtle, S. (2020). In and Out of the Bursa—The Role of CXCR4 in Chicken B Cell Development. *Front. Immunol.* **11**, 1–18.

Nagy, N., Oláh, I. and Vervelde, L. (2022). Structure of the avian lymphoid system. In *Avian Immunology*, pp. 11–44. Elsevier.

Nakamura-Ishizu, A., Okuno, Y., Omatsu, Y., Okabe, K., Morimoto, J., Uede, T., Nagasawa, T., Suda, T. and Kubota, Y. (2012). Extracellular matrix protein tenascin-C is required in the bone marrow microenvironment primed for hematopoietic regeneration. *Blood* **119**, 5429–5437.

Neely, H. R. and Flajnik, M. F. (2016). Emergence and Evolution of Secondary Lymphoid Organs. *Annu. Rev. Cell Dev. Biol.* **32**, 693–711.

Olah, I. and Glick, B. (1978). The Number and Size of the Follicular Epithelium (FE) and Follicles in the Bursa of Fabricius. *Poult. Sci.* **57**, 1445–1450.

Oláh, I. and Nagy, N. (2013). Retrospection to discovery of bursal function and recognition of avian dendritic cells; Past and present. *Dev. Comp. Immunol.* **41**, 310–315.

Oláh, I., Glick, B. and Törö, I. (1986). Bursal Development in Normal and Testosterone-Treated Chick Embryos. *Poult. Sci.* **65**, 574–588.

Olah, I., Kendall, C. and Glick, B. (1992). Differentiation of bursal secretory-dendritic cells studied with anti-vimentin monoclonal antibody. *Anat. Rec.* **233**, 111–120.

Oláh, I., Felföldi, B., Benyeda, Z., Nagy, N. and Kovács, T. (2022). The morphology and differentiation of stromal cells in the cortex of follicles in the bursa of Fabricius of the chicken. *Anat. Rec.* **305**, 3297–3306.

Onder, L., Mörbe, U., Pikor, N., Novkovic, M., Cheng, H. W., Hehlgans, T., Pfeffer, K., Becher, B., Waisman, A., Rülicke, T., et al. (2017). Lymphatic Endothelial Cells Control Initiation of Lymph Node Organogenesis. *Immunity* **47**, 80-92.e4.

Paramithiotis, E. and Michael, J. H. R. (1994). B cell emigration directly from the cortex of lymphoid follicles in the bursa of Fabricius. *Eur. J. Immunol.* **24**, 458–463.

Paramithiotis, E. and Ratcliffe, M. J. H. (1993). Bursa-dependent subpopulations of peripheral B lymphocytes in chicken blood. *Eur. J. Immunol.* **23**, 96–102.

Paramithiotis, E. and Ratcliffe, M. J. (1994). Survivors of bursal B cell production and emigration. *Poult. Sci.* **73**, 991–997.

Paramithiotis, E. and Ratcliffe, M. J. H. (1996). Evidence for Phenotypic Heterogeneity Among B Cells Emigrating from the Bursa of Fabricius: A Reflection of Functional Diversity?pp. 29–36.

Parvari, R., Avivi, A., Lentner, F., Ziv, E., Tel-Or, S., Burstein, Y. and Schechter, I. (1988). Chicken immunoglobulin gamma-heavy chains: limited VH gene repertoire, combinatorial diversification by D gene segments and evolution of the heavy chain locus. *EMBO J.* **7**, 739–744.

Patel, A., Harker, N., Moreira-Santos, L., Ferreira, M., Alden, K., Timmis, J., Foster, K., Garefalaki, A., Pachnis, P., Andrews, P., et al. (2012). Differential RET signaling pathways drive development of the enteric lymphoid and nervous systems. *Sci. Signal.* **5**, 1–11.

Pharr, T., Olah, I., Bricker, J., Olson, W. C., Ewert, D., Marsh, J. and Glick, B. (1995a). Characterization of a novel monoclonal antibody, EIV-E12, raised against enriched splenic ellipsoid-associated cells. *Hybridoma* **14**, 51–57.

Pharr, T., Olah, I., Bricker, J., Olson, W. C., Ewert, D., Marsh, J. and Glick, B. (1995b). Characterization of a novel monoclonal antibody, EIV-E12, raised against enriched splenic ellipsoid-associated cells. *Hybridoma* **14**, 51–57.

Pink, J. R., Vainio, O. and Rünbeek, A. -M (1985). Clones of B lymphocytes in individual follicles of the bursa of Fabricius. *Eur. J. Immunol.* **15**, 83–87.

Pospisil, R. and Mage, R. G. (2011). Rabbit Appendix: A Site of Development and Selection of the B Cell Repertoire. 59–70.

Pourquié, O., Coltey, M., Thomas, J.-L. and Le Douarin, N. M. (1990). A widely distributed antigen developmentally regulated in the nervous system. *Development* **109**, 743–752.

Quesada, J. and Agulleiro, B. (1984). Ultrastructure of granulopoiesis in tunica propria of the bursa of fabricius. *Dev. Comp. Immunol.* **8**, 219–224.

Ratcliffe, M. J. H. (2006). Antibodies, immunoglobulin genes and the bursa of Fabricius in chicken B cell development. *Dev. Comp. Immunol.* **30**, 101–118.

Ratcliffe, M. J. H. and Härtle, S. (2022). B cells, the bursa of Fabricius, and the generation of antibody repertoires. In *Avian Immunology*, pp. 71–99. Elsevier.

Rennert, P. D., James, D., Mackay, F., Browning, J. L. and Hochman, P. S. (1998). Lymph Node Genesis Is Induced by Signaling through the Lymphotoxin β Receptor. *Immunity* **9**, 71–79.

Reynaud, C. (1985). A single rearrangement event generates most of the chicken immunoglobulin light chain diversity. *Cell* **40**, 283–291.

Reynaud, C.-A., Anquez, V., Grimal, H. and Weill, J.-C. (1987). A hyperconversion mechanism generates the chicken light chain preimmune repertoire. *Cell* **48**, 379–388.

Reynaud, C.-A., Dahan, A., Anquez, V. and Weill, J.-C. (1989). Somatic hyperconversion diversifies the single VH gene of the chicken with a high incidence in the D region. *Cell* **59**, 171–183.

Reynaud, C. A., Mackay, C. R., Müller, R. G. and Weill, J. C. (1991). Somatic generation of diversity in a mammalian primary lymphoid organ: The sheep ileal Peyer's patches. *Cell* **64**, 995–1005.

Reynaud, C.-A., Bertocci, B., Dahan, A. and Weill, J.-C. (1994). Formation of the Chicken B-Cell Repertoire: Ontogenesis, Regulation of Ig Gene Rearrangement, and Diversification by Gene Conversion.pp. 353–378.

Riddle, R. D., Johnson, R. L., Laufer, E. and Tabin, C. (1993). Sonic hedgehog mediates the polarizing activity of the ZPA. *Cell* **75**, 1401–1416.

Ruddle, N. H. (2025). From Lymphotoxin to Tertiary Lymphoid Structures and Beyond. *Immunol. Rev.* **335**,.

Sawa, S., Cherrier, M., Lochner, M., Satoh-Takayama, N., Fehling, H. J., Langa, F., Di Santo, J. P. and Eberl, G. (2010). Lineage Relationship Analysis of RORγt Innate Lymphoid Cells. *Science (1979).* **330**, 665–669.

Sayegh, C. E., Demaries, S. L., Pike, K. A., Friedmann, J. E. and Ratcliffe, M. J. H. (2000). The chicken B-cell receptor complex and its role in avian B-cell development. *Immunol. Rev.* **175**, 187–200.

Schneider, K., Kothlow, S., Schneider, P., Tardivel, A., Göbel, T., Kaspers, B. and Staeheli, P. (2004). Chicken BAFF - A highly conserved cytokine that mediates B cell survival. *Int. Immunol.* **16**, 139–148.

Schulz, O., Hammerschmidt, S. I., Moschovakis, G. L. and Förster, R. (2016). Chemokines and Chemokine Receptors in Lymphoid Tissue Dynamics. *Annu. Rev. Immunol.* **34**, 203–242.

Sécca, C., Bando, J. K., Fachi, J. L., Gilfillan, S., Peng, V., Luccia, B. Di, Cella, M., McDonald, K. G., Newberry, R. D. and Colonna, M. (2021). Spatial distribution of LTi-like cells in intestinal mucosa regulates type 3 innate immunity. *Proc. Natl. Acad. Sci. U. S. A.* **118**, 1–9.

Shikhagaie, M. M., Björklund, Å. K., Mjösberg, J., Erjefält, J. S., Cornelissen, A. S., Ros, X. R., Bal, S. M., Koning, J. J., Mebius, R. E., Mori, M., et al. (2017). Neuropilin-1 Is Expressed on Lymphoid Tissue Residing LTi-like Group 3 Innate Lymphoid Cells and Associated with Ectopic Lymphoid Aggregates. *Cell Rep.* **18**, 1761–1773.

Shiojiri, N. and Takahashi, M. (1991). Lymphoid follicle formation in the bursa of Fabricius of the chick embryo. *J. Anat.* **175**, 237–249.

Simic, M., Manosalva, I., Spinelli, L., Gentek, R., Shayan, R. R., Siret, C., Girard-Madoux, M., Wang, S., de Fabritus, L., Verschoor, J., et al. (2020). Distinct Waves from the Hemogenic Endothelium Give Rise to Layered Lymphoid Tissue Inducer Cell Ontogeny. *Cell Rep.* **32**, 108004.

Soos, G., Olah, I., Kittner, Z., Toro, I. and Glick, B. (1990). Effect of the progestogen, allylestriol, on the bursal development of the chicken. *Dev. Comp. Immunol.* **14**, 457–463.

Soós, Á., Szőcs, E., Halasy, V., Jurenka, C. and Nagy, N. (2025). Tenascin-C regulates CXCR4+ B cell migration and cortex formation in the developing bursa of Fabricius. *Front. Immunol.* **16**,.

Szőcs, E., Balic, A., Soós, Á., Halasy, V. and Nagy, N. (2024). Characterization and ontogeny of a novel lymphoid follicle inducer cell during development of the bursa of Fabricius. *Front. Immunol.* **15**,.

Thompson, C. B. and Neiman, P. E. (1987). Somatic diversification of the chicken immunoglobulin light chain gene is limited to the rearranged variable gene segment. *Cell* **48**, 369–378.

Ting-Berreth, S. A. and Chuong, C. M. (1996). Sonic hedgehog in feather morphogenesis: Induction of mesenchymal condensation and association with cell death. *Developmental Dynamics* **207**, 157–170.

Toivanen, P. and Toivanen, A. (1973). Bursal and postbursal stem cells in chicken. functional characteristics. *Eur. J. Immunol.* **3**, 585–595.

van de Pavert, S. A. (2021). Lymphoid Tissue inducer (LTi) cell ontogeny and functioning in embryo and adult. *Biomed. J.* **44**, 123–132.

van de Pavert, S. A. (2023). Layered origins of lymphoid tissue inducer cells. *Immunol. Rev.* **315**, 71–78.

Van De Pavert, S. A., Olivier, B. J., Goverse, G., Vondenhoff, M. F., Greuter, M., Beke, P., Kusser, K., Höpken, U. E., Lipp, M., Niederreither, K., et al. (2009). Chemokine cxcl13 is essential for lymph node initiation and is induced by retinoic acid and neuronal stimulation. *Nat. Immunol.* **10**, 1193–1199.

van de Pavert, S. A., Ferreira, M., Domingues, R. G., Ribeiro, H., Molenaar, R., Moreira-Santos, L., Almeida, F. F., Ibiza, S., Barbosa, I., Goverse, G., et al. (2014). Maternal retinoids control type 3 innate lymphoid cells and set the offspring immunity. *Nature* **508**, 123–127.

Veiga-Fernandes, H., Coles, M. C., Foster, K. E., Patel, A., Williams, A., Natarajan, D., Barlow, A., Pachnis, V. and Kioussis, D. (2007). Tyrosine kinase receptor RET is a key regulator of Peyer's Patch organogenesis. *Nature* **446**, 547–551.

Velaga, S., Herbrand, H., Friedrichsen, M., Jiong, T., Dorsch, M., Hoffmann, M. W., Förster, R. and Pabst, O. (2009). Chemokine Receptor CXCR5 Supports Solitary Intestinal Lymphoid Tissue Formation, B Cell Homing, and Induction of Intestinal IgA Responses. *The Journal of Immunology* **182**, 2610–2619.

Vivier, E., Artis, D., Colonna, M., Diefenbach, A., Di Santo, J. P., Eberl, G., Koyasu, S., Locksley, R. M., McKenzie, A. N. J., Mebius, R. E., et al. (2018). Innate Lymphoid Cells: 10 Years On. *Cell* **174**, 1054–1066.

von La Roche, D., Schumacher, M., Kohn, M., Trapp, J., Schusser, B., Rautenschlein, S. and Härtle, S. (2024). Characterization of class-switched B cells in chickens. *Front. Immunol.* **15**, 1–22.

Weill, J. C., Reynaud, C. A., Lassila, O. and Pink, J. R. L. (1986). Rearrangement of chicken immunoglobulin genes is not an ongoing process in the embryonic bursa of Fabricius. *Proc. Natl. Acad. Sci. U. S. A.* **83**, 3336–3340.

Wilson, T. J. and Boyd, R. L. (1990). Cyclophosphamide- and testosterone-induced alteration in chicken bursal stroma identified by monoclonal antibodies. *Immunology* **70**, 241–6.

Wu, Z., Harne, R., Idoko-Akoh, A., Foschi, F., Meddle, S. L., Macdonald, J., Shih, B., Mcgrew, M., Hume, D. A. and Balic, A. (2026). CSF1R-dependent macrophages control B cell development and function in the chicken immune system.

Yasuda, M., Jenne, C. N., Kennedy, L. J. and Reynolds, J. D. (2006). The sheep and cattle Peyer's patch as a site of B-cell development. *Vet. Res.* **37**, 401–415.

Yvernogeau, L. and Robin, C. (2017). Restricted intra-embryonic origin of bona fide hematopoietic stem cells in the chicken. *Development (Cambridge)* **144**, 2352–2363.

Yvernogeau, L., Nagy, N., Dunon, D., Robin, C. and Jaffredo, T. (2022). Development of the avian hematopoietic and immune systems. In *Avian Immunology*, pp. 45–69. Elsevier.

Zipfel, P. F. and Skerka, C. (2022). From magic bullets to modern therapeutics: Paul Ehrlich, the German immunobiologist and physician coined the term ‘complement.’ *Mol. Immunol.* **150**, 90–98.

9. BIBLIOGRAPHY OF THE CANDIDATE'S PUBLICATIONS

9.1. List of publications related to the thesis

Szőcs, E., Balic, A., Soós, Á., Halasy, V., and Nagy, N. (2024). Characterization and ontogeny of a novel lymphoid follicle inducer cell during development of the bursa of Fabricius. *Frontiers in Immunology*, 15:1449117.
IF: 5,9

Soós, Á.*, **Szőcs, E.***, Halasy, V., Jurenka, C., and Nagy, N. (2025). Tenascin-C regulates CXCR4+ B cell migration and cortex formation in the developing bursa of Fabricius. *Frontiers in Immunology*, 16:1636140.
*Contributed equally.
IF: 7,0

9.2. List of own publications not related to the thesis

Roche, D.L.; Naumann, I.; **Szőcs, E.**; Halasy, V.; Kohn, M.; Kaspers, B.; Nagy, N.; Härtle, S. (2026). Characterization of Harderian Gland-Derived Plasma Cells in Chicken. *European Journal of Immunology.* 56(6):70214.

IF: 4,1

Soós, Á.; **Szőcs, E.**; Halasy, V.; Gecse, Zs.; Mógor, F.; Jurenka, C.; Kocsis, K.; Mucksová, J.; Hejnar, J.; Nagy, N. (2025). Cecal growth factors promote enteric neurosphere formation and hindgut colonization in the avian model. *Frontiers in Cell and Developmental Biology,* 13:1681844.

IF: 5,3

Dora, D.; **Szőcs, E.**; Soós, Á.; Halasy, V.; Somodi, C.; Mihucz, A.; Rostás, M.; Mógor, F.; Lohinai, Z.; Nagy, N. (2024). From bench to bedside: an interdisciplinary journey through the gut-lung axis with insights into lung cancer and immunotherapy. *Frontiers in Immunology,* 15:1434804.

IF: 5,9

Molnár, M.; Lázár, B.; Sztán, N.; Végi, B.; Drobnyák, Á.; Buda, K.; Nagy, N.; **Szőcs, E.**; Pecsenye-Fejszák, N.; Liptói, K.; Gócza, E.; McGrew, M.J.; Várkonyi, E. (2024). Successful formation of sperm cells from transplanted primordial germ cells in sterile interspecific avian recipients. *Scientific Reports*, 14(1):24678.

IF: 3,9

Oláh, I.; Felföldi, B.; Benyeda, Z.; Magyar, A.; Nagy, N.; Soós, Á.; **Szőcs, E.** (2024). Life cycle of chicken bursal secretory dendritic cell (BSDC). *Poultry Science*, 103(6):103640.

IF: 4,2

Halasy, V.; **Szőcs, E.**; Soós, Á.; Kovács, T.; Pecsenye-Fejszák, N.; Hotta, R.; Goldstein, A. M.; Nagy, N. (2023). CXCR4 and CXCL12 signaling regulates the development of extrinsic innervation to the colorectum. *Development,* 150(8):dev201289.
IF: 3,7

Kovács, T.*; Halasy, V.*; Pethő, C.; **Szőcs, E.**; Soós, Á.; Dóra, D.; de Santa Barbara P.; Faure, S.; Stavely, R.; Goldstein, A.M.; Nagy, N. (2023). Essential Role of BMP4 Signaling in the Avian Ceca in Colorectal Enteric Nervous System Development, *International Journal of Molecular Sciences,* 24(21):15664.
* Contributed equally.
IF: 4,9

Oláh, I.; Felföldi, B.; Benyeda, Z.; Nagy, N.; Magyar, A.; Szőcs, E.; Soós, Á. (2023). Effect of Intermediate Plus Vaccine and vvIBDV on Bursa Secretory Cells and Their Glycoprotein Production. *Viruses*, 15(6):1301.
IF: 3,8

Omer, S.; Nagy, N.; **Szőcs, E.**; Kádár, S.; Völgyi, G.; Pinke, B.; Mészáros, L.; Katona, G.; Vincze, A.; Dormán, P.; Nagy Z. Zs.; Balogh G.T.; Kazsoki A.; Zelkó R. (2023). Development of innovative electrospun nepafenac-loaded nanofibers-based ophthalmic inserts. *International Journal of Pharmaceutics,* 647: 23554.
IF: 5,3

Stavely, R.; Hotta, R.; Guyer, R. A.; Picard, N.; Rahman, A. A.; Omer, M.; Soos, A.; **Szocs, E.**; Mueller, J.; Goldstein, A. M.; Nagy, N. (2023). A distinct transcriptome characterizes neural crest-derived cells at the migratory wavefront during enteric nervous system development. *Development,* 150(5):201090.
IF: 3,7

Fejszák, N.; Kocsis, K.; Halasy, V.; **Szőcs, E.**; Soós, Á.; Roche, D. L.; Härtle, S.; Nagy, N. (2022). Characterization and functional properties of a novel monoclonal antibody which identifies a B cell subpopulation in bursa of Fabricius. *Poultry Science*, 101(4):101711.
IF: 4,4

Nagy, N.; Kovács, T.; Stavely, R.; Halasy, V.; Soós, Á.; **Szőcs, E.**; Hotta, R.; Graham, H.; Goldstein, A.M. (2021). Avian ceca are indispensable for hindgut enteric nervous system development. *Development,* 148(22):dev199825.
IF: 6,8

10. ACKNOWLEDGMENTS

I would like to express my sincere gratitude to my supervisor, Prof. Dr. Nándor Nagy, who first introduced me to developmental biology during my undergraduate years. His professional guidance, patience, and enthusiasm enabled me to pursue this journey and shaped me both as a person and an aspiring scientist.

I am grateful to Prof. Dr. Alán Alpár, Director of the Department of Anatomy, Histology and Embryology, for providing the opportunity to undertake my doctoral studies within the department.

I would like to thank Dr. Ildikó Bódi for reviewing my dissertation and providing valuable critical remarks, which were instrumental in completing this work.

I am especially thankful to my fellow PhD students and friends, Ádám Soós and Dr. Viktória Gáspár-Halasy, for our countless brainstorming sessions and for making long hours in the lab feel remarkably short. I could not have asked for better partners on this journey.

I would like to thank Dr. Katalin Szászné Kocsis and Dr. Nóra Pecsenye-Fejszák, who offered constant support not only in my teaching duties, but also in all aspects of academic life.

Furthermore, I would like to thank all current and former members of the Stem Cell and Experimental Embryology Laboratory for their expertise and valuable friendship throughout my PhD years: Bettina Kaczur, Noémi Kegyes, Csenge Jurenka, Zsófia Bogya, Zsanna Gecse, Tíra Panna Katona, Réka Borbála Tóth, Fruzsina Mógor, Dr. Krisztina H. Minkó, Györgyné Vidra, Dr. Dávid Dóra, Dr. Tamás Kovács.

Last but not least, I am forever grateful to my parents and my friends, whose unwavering support and belief in me allowed me to complete my PhD journey with a smile on my face.